Data Access Requirements Document (DARD)

Prepared by: Glaciers_cci consortium
Contract: 4000101778/10/I-AM
Name: Glaciers_cci-D1.3_DARD
Version: 1.0
Date: 20.11. 2011

Contact:
Frank Paul
Department of Geography
University of Zurich
frank.paul@geo.uzh.ch

Technical Officer:
Stephen Plummer
ESA ESRIN

Document status sheet

Version	Date	Changes	Approval
v0.2	10.05.2011		
v0.5	31.07.2011	contrib. from GUIO added	
V0.6	16.08.2011	contrib. from SEEL added	
v0.7	5.11. 2011	corrections from technical officer considered	
v1.0	20.11 2011	final comments from TO to revised version included	

The work described in this report was done under ESA contract 4000101778/10/I-AM. Responsibility for the contents resides in the authors that prepared it.

Author team:
Frank Paul (GIUZ), Andreas Kääb, Christopher Nuth (GUIO), Thomas Nagler, Helmut Rott, Killian Scharrer (Enveo), Andrew Shepherd, Francesca Ticconi (SEEL), Tazio Strozzi (Gamma)

Glaciers_cci Technical Officer at ESA:
Stephen Plummer

Contents

1. Overview

1.1 Purpose of the document

This is the Data Access Requirements Document (DARD) of the Glaciers_cci project. It is the third and final deliverable of Task 1 (D1.3). In agreement with the Statement of Work (SoW) it lists 'all the data, including all EO, ancillary and validation data, that are needed to perform the project. In more detail, 'The DARD shall include detailed requirements for resolving any known data access, calibration, validation and performance issues specific to the satellite ground segment processing and identify potential algorithm upgrades enabling the regeneration of improved and most accurate input products required for each ECV.' As the EO data used in the Glaciers_cci project do not require to change the satellite ground segment processing (i.e. data will be used 'as is'), we focus here on the technical details of the sensors required to generate the products as described in the PSD (Glaciers_cci, 2011b), their availability and their access conditions (e.g. licences). Due to the constantly growing archives, the ongoing activities of the GLIMS participants, and the user requirement to use only the most appropriate data sets for product generation and validation, we will focus on the spatial coverage by listing path/row of the EO data (including SAR, optical satellite data and altimeter data) of the key regions rather than listing all the available dates of image acquisition. By browsing through the EO data archives, e.g. glovis, EOLI etc., we found a sufficient number of appropriate scenes for the selected key regions to reach the project goals.

We start with a short description of the key regions and provide some background on product validation and the round robin to be performed in Task 2, to better understand the reasons for selecting and describing the respective datasets here. We then provide the details for each of the three products glacier area, elevation change and velocity fields. Each product chapter is structured in the four sections EO data for (1) product generation and (2) validation and (3) auxiliary data for product generation and (4) validation. Each of these four sections is again subdivided into three sections data sources, data availability and data access conditions. As the satellite data used to generate each of the products are largely different, the sorting for products is very practical, in particular for the reader interested in a specific product. However, in very rare cases a description of a specific data set has been given earlier, and only the related section is referenced.

1.2 Reference documents

Though this document has several tables summarizing sensor characteristics, we have made extensive use of hyperlinks to reference documents where full details that are available in the web. We are sure that this will strongly increase the readability of this document without loss of detail. A summary of the main web pages for data access and detailed data descriptions is provided in Appendix 1 and will also be available on the Glaciers_cci webpage. When additional useful links will emerge, we will add them on the webpage.

2. Key regions

The preliminary list of key regions for **product generation** is described in Table 3 of the URD (Glaciers_cci, 2011a). Due to the ongoing activities by other groups, the list is subject to frequent change. In the following, we focus on the regions selected for **product validation** and the **round robin** experiments (Table 2.1). We distinguish the two mainly due to different data access conditions and the different purposes. While all data for the round-robin experiments must be freely available, the datasets that are used for product validation are in some cases restricted in their availability (e.g. DEMs from national agencies or high resolution satellite data). With the round robin experiments focussing on algorithm application and later selection, the validation has one focus on assessing product accuracy. The EO team and the CRG of the project will be involved in both activities and the wider glaciological community will be invited to participate in the round-robin experiments. Their set-up and the validation activities will be slightly different for each product. We thus describe here the key regions for both investigations separated by product.

	Validation			Round Robin		
Region	**area**	**elev. ch.**	**velocity**	**area**	**elev. ch.**	**velocity**
Alaska				X		
Iceland (Vatnajøkul)			X			
Svalbard (Kronebreen)		X	X			X
Austfonna/Vestfonna		X	X			X
Norway	X					
Alps	X	X		X	X	
Himalaya (Khumbu)	X					
Himalaya (Karakoram)				X	X	X

Table 2.1: Overview of the key regions selected for product validation and the round robin for each of the products (elev. ch. = elevation change).

2.1 Glacier area

2.1.1 Product validation

As detailed in section 3.2.1, product validation will be performed by internal and external measures. The internal validation is basically a multiple digitizing of the same set of glaciers that will also be performed as a part of the algorithm comparison in the round-robin experiments (see 2.1.2). The external validation will compare the satellite-derived glacier outlines (with and without editing) with higher resolution data sets, basically by comparing the derived glacier areas as determined from a manual digitization of the outlines. The key regions selected for product validation include the Alps, Norway, and the Himalaya (see Table 2.1). Glaciers of different types can be found in these regions resulting in a wide range of challenges for glacier mapping. Validation data from high-resolution sensors and independently digitized glaciers outlines are avaialble as well. Through Google Earth™ it is possible to obtain screen-shots from high-resolution sensors (incl. aerial photography) for product validation in nearly any region in the world (Fig. 2.1). After iterative geocoding of the upper left corner and determination of the pixel size, they can be used in the same way as (self-geocoded) raw data. Several of them will be used in Glaciers_cci for product validation.

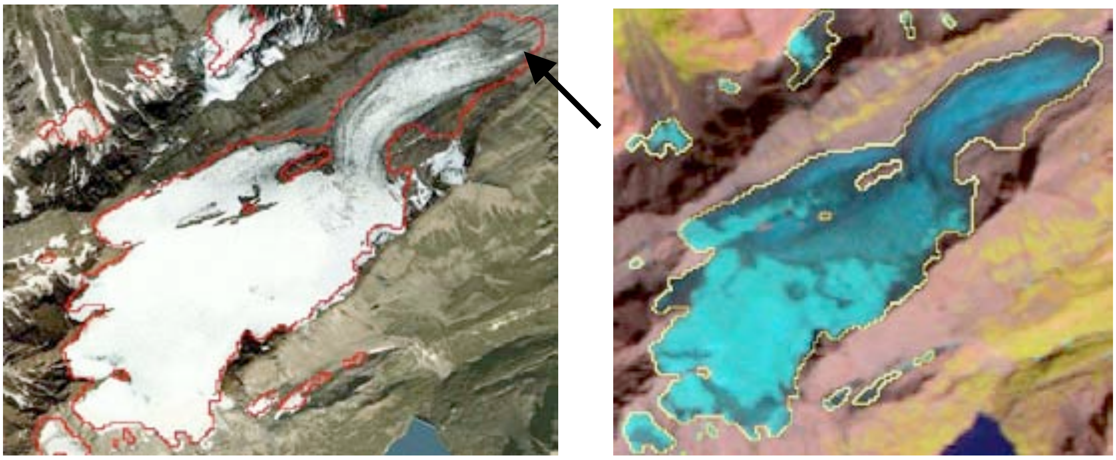

Fig. 2.1: Overlay of glacier outlines (red and yellow) derived from a Landsat TM scene of 2003 for Griesglacier (Switzerland) with an aerial photograph from 2010 (left) and the original TM image (band 5, 4, 3 composite, right). The left image is an iteratively geocoded screen shot from Google Maps showing the retreat of Gries glacier in 7 years (arrow). Snow conditions are not optimal, but still acceptable to map the extent of the largest glacier.

2.1.2 Round Robin experiments

The key regions for the round-robin experiments will be very similar to the validation sites, but the specific glaciers selected are partially different. For the algorithm comparisons we will select test sites in Alaska, the Alps and the Himalayas (Table 2.1). They will reflect a wide range of glacier types (cirque, mountain, valley, icecap), conditions (with debris cover, shadow, clouds, lakes, seasonal snow), and sizes (from small to large). Additionally, a couple of glaciers in different parts of the world (likely those mentioned above) will be used for multiple digitizing experiments. This includes images from different sensors (Landsat-type and high-resolution), and glaciers of different size and type.

2.2 Elevation change

2.2.1 Product validation

Product validation will be based on internal and external measures. While the internal measures rely on the data themselves, the external measures require additional data. The most important measure for internal validation will be the co-registration procedure for multiple elevation data. This is completely independent of the type of elevation data as long as they are spatially distributed. The procedure provides shifts between the data, their relative accuracy for stable ground, possible elevation trends with elevation, and possible higher-order errors in the data. The procedure is not dependent on the region where the data will be validated as long as there is stable ground contained with a variety of slopes and aspects. External validation of elevation changes requires independent and, if possible, more accurate elevation sources than the ones used for production. External validation will be performed where suitable validation data are available, i.e. on Svalbard and in the European Alps (Table 2.1).

2.2.2 Round Robin experiments

The key regions for the round robin experiments on elevation changes will represent a wide range of glaciological characteristics, climatic zones, and topographic and surface types (polar, high mountain, clean ice, snow/firn, debris cover, small glaciers, big glaciers, etc.).

Also, the sites are representative in terms of production data available (SPOT5 SPIRIT, SRTM, ASTER, ASTER GDEM, ICESat, etc.). The currently most probable sites for this are the Himalaya and the Alps. The round robin experiments to be performed will consist of:

- Pre-processing: Check the co-registration. There are a few methods to do this. What do the participants apply? What is the mean bias correction between two given DEMs?
- Post-processing: How is the filtering to remove spurious elevation changes done (mainly relevant for DEM differencing)? How does this affect the final elevation changes (i.e. elevation changes per elevation bin).

2.3 Velocity

2.3.1 Product validation

Strict independent product validation for glacier velocities derived from air and space data is a difficult task because it would require reference measurements of exactly the same time. Due to short-term and seasonal velocity variations of glaciers, even small differences in the observation time window might introduce significant velocity differences. In addition, point measurements such as ground measurements represent a different surface area (points) than satellite measurements (averaging over pixel windows). Similar to the above external validation approaches by reference measurements, a number of internal validation measures are available, but also all of these are not completely conclusive, and provide only indications. We base our validations therefore on combinations of different measures.

An important site for external velocity validation will be Kronebreen (Svalbard), where repeat medium resolution and high resolution SAR and optical data from similar time windows are available together with ground-based GPS measurements, recently even continuous GPS. Such data are also available from Austfonna and Vestfonna. In particular, for the Vestfonna Ice Cap a geodetic campaign was performed between 2007 and 2010 in order to estimate the ice velocity field within the framework of the IPY project KINNVIKA (Pohjola et al., in press). Data from this project are available for Glaciers_cci. Ice surface velocities from geodetic measurements are available for 23 fixed stations. For the third validation site Vatnajøkull (Iceland) high-resolution satellite (TerraSAR-X) and GPS data are available.

Internal validation measures do not depend on the validation location and can freely be chosen to represent the glacier characteristics found in the regions selected for product generation.

2.3.2 Round Robin experiments

Only few scientists are expected to test velocity algorithms on provided image data for a round robin. Rather, scientists will use velocity data (perhaps using different algorithms) to analyse their usefulness for a specific application. We will thus provide a set of methods along with the raw data for application by the participants. In contrast to the other two products, the focus of the round robin is here on algorithm cross-comparison. The test sites will be similar to the regions selected for the other products to benefit from potential synergies and to facilitate combined judgement of the data. The selected locations currently include Svalbard (Kronebreen and Austfonna/Vestfonna) and the Karakoram region in the Himalaya (Table 2.1).

3. Glacier area

3.1 EO data for product generation

3.1.1 Data sources

The glacier area product consists of two parts:

(1) the glacier outline as mapped from the specified sensors, and

(2) the glacier inventory data that can only be created when additionally a DEM (auxiliary data) is available.

For the purpose of creating a glacier inventory (2) on a global scale, it is mandatory to have free and easy data access to both the satellite imagery and the DEM, and it is beneficial when the data can be used as they are, e.g. without the further need for orthorectification. With glaciers and icecaps spanning 6 orders of magnitude in size (from 0.01 to 10000 km^2), it is required for efficient and complete mapping that the sensor covers large regions with sufficiently high resolution. The freely available and already orthorectified Landsat data from USGS (L1T product) fulfil these requirements in the best possible way. They do thus form the core data set for generation of the area product on a global scale. However, this does not imply that other sensors with similar spectral characteristics cannot be used. In particular the huge (and still growing) archives of ASTER and SPOT scenes are suitable as well. They just require a higher processing workload due to the smaller area covered (about 1/9 of Landsat) and the required orthorectification. They are thus more suitable for specific studies (e.g. the velocity product) than for global mapping. In the near future Sentinel-2 data will be an ideal sensor for glacier outline mapping.

The core of the automated glacier mapping relies on the availability of a sensor with bands in the visible (VIS; between 0.4 to 0.8 μm) and shortwave infrared (SWIR; around 1.6 μm) part of the spectrum. Due to the different spectral characteristics of glacier ice and snow in the VIS (where both have high reflectance) and SWIR (where both absorb most of the radiation), a simple band ratio with a threshold allows a pixel sharp classification (e.g. Paul and Kääb, 2005). Unfortunately, a SWIR band is not available from high-resolution sensors. They are often only panchromatic, or at best have a band in the near infrared. This can significantly reduce the quality of the glacier outlines derived from high-resolution data, in particular in the case of low optical contrast (e.g. between bare ice and the surrounding rock). Key sensor characteristics for the glacier area product are:

- optical sensors with a spatial resolution of 30 m or better,
- sufficient swath width for fully covering large glaciers (e.g. Landsat Type),
- a VIS and SWIR band (for cloud versus snow/ice detection),
- an acquisition strategy suitable for monitoring glaciers (e.g. at the end of summer with maximum ablation), and
- free access to data.

An additional sensor that has proven to be useful for the precise delineation of debris- covered glaciers (based on coherence images) is ALOS PALSAR. Though, coherence images (taken over summer) are not mandatory for product generation, they make delineation of debris-covered glaciers more certain, in particular in regions with low optical contrast. In this regard they are seen as auxiliary EO data for the glacier area product. The detailed description of this sensor is given in section 5.1.2 along with all other microwave sensors. In Tables 3.1 to 3.3

we summarize the key characteristics of the most suitable current optical sensors (Landsat TM/ETM+, Terra ASTER, SPOT HRV, IRS1C/D) along with the specifications of two future sensors (Sentinel 2 MSI and Landsat OLI). We summarize the important spectral ranges and spatial resolution (Table 3.1), the key applications in Glaciers_cci (Table 3.2), and special characteristics of the respective missions (Table 3.3).

All satellite data are used as they are, i.e. system corrected and orthorectified (USGS L1T). Product generation uses raw digital numbers (DNs), i.e. they are neither converted to spectral reflectance or albedo, nor are they corrected for atmospheric or topographic effects. For selected regions the central part of the Landsat 7 ETM+ data with the scan line corrector failure are used as well.

TM/ETM+ band (spectral region)	Landsat TM	Landsat ETM+	Terra ASTER	SPOT 4 HRV	IRS-1C/D LISS 3	Sentinel 2 MSI	LDCM OLI
1 (blue)	0.45-0.52	0.45-0.52	-	-	-	0.46-0.52	0.45-0.52
2 (green)	0.52-0.60	0.53-0.61	0.52-0.60	0.52-0.59	0.52-0.59	0.54-0.58	0.53-0.60
3 (red)	0.63-0.69	0.63-0.69	0.63-0.69	0.61-0.68	0.63-0.68	0.65-0.68	0.63-0.68
4 (NIR)	0.76-0.90	0.76-0.90	0.76-0.86	0.78-0.89	0.77-0.86	0.78-0.90	0.85-0.89
5 (SWIR)	1.55-1.75	1.55-1.75	1.60-1.70	1.58-1.75	1.55-1.70	1.57-1.65	1.56-1.66
7 (SWIR)	2.08-2.35	2.09-2.35	2.15-2.43[1]	-	-	2.1-2.3	2.1-2.3
6 (therm)	10.4-12.5	10.4-12.5	10.25-11.65	-	-	-	10.3-12.5[2]
8 (pan)	-	0.52-0.90	-	0.51-0.73	0.50-0.75	-	0.5-0.68

Table 3.1: Spectral band ranges of the sensors that are suitable for creation of the glacier area product. The spatial resolution (in m) is colour-coded: 10, 15, 20, 30, 60, 90, 120. NIR: near infrared, SWIR: short wave infrared, therm: thermal infrared, pan: panchromatic, [1]: 5 bands, [2]: 2 bands. Sources: http://landsat.usgs.gov/band_designations_landsat_satellites.php, http://geo.arc.nasa.gov/sge/health/sensor/cfsensor.html, and ESA (2010).

TM/ETM+ band	Applications
1 (blue)	For mapping and identification of ice and snow in cast shadow and automated lake detection, often saurated over snow, part of band 3,2,1 composite
2 (green)	Alternative for band 1 for ASTER, SPOT, LISS3, part of band 3,2,1 and 4,3,2 composite
3 (red)	Main input for band ratio (TM3/TM5) and part of band 3, 2, 1 and 5, 4, 3 composites
4 (NIR)	Best contrast over snow, alternative for band 3, part of FCC with bands 5,4,3
5 (SWIR)	Main input for band ratio (TM3/TM5) and FCC with bands 5,4,3
6 (therm)	Alternative for band 5 in regions with thin volcanic ash layers, but has lower spatial resolution
8 (pan)	poor contrats bare ice vs. rock, most useful for feature tracking (velocity product)

Table 3.2: Typical applications of the spectral bands in Glaciers_cci.

Characteristic	Landsat TM	Landsat ETM+	Terra ASTER	SPOT 4 HRV	IRS-1C/D LISS 3	Sentinel 2 MSI	LDCM OLI
Launch	1984	1999	1999	1998	1995	2014	2013
Swath width [km]	185	185	60	60	145	290	185
Repeat cycle [days]	16 (8[1])	16 (8[1])	16[2]	3	24		16
Equator crossing time [UT]	9:30	10:00	10:30	10:30	10:30		
Max. Latitude [°]	82	82	83				

Table 3.3: Main orbit characteristics of the sensors suitable for creation of the glacier area product. [1]: 8 days if Landsat 5 and 7 are used, [2]: Terra follows Landsat but ASTER can point within a scene. Sources: http://geo.arc.nasa.gov/sge/health/sensor/cfsensor.html

The temporal coverage of data availability for the sensors listed in Tables 3.1 and 3.3 is given in Table 3.4. Only sensors with a SWIR band are considered in this selection. Landsat 5 has by far the largest temporal coverage, but scenes are not available in each year for each region.

In summary, the data requirements for product generation are:
- optical EO data with at least 30 m spatial resolution and one band in the SWIR
- large spatial coverage, sun-synchronous orbit, nadir view preferable
- free access to orthorectified (accuracy: 1 pixel RMSE) and system corrected data
- data will be used as they are (raw DNs), no atmospheric or terrain correction will be applied
- a DEM of sufficient quality is required to create the level 2 product (glacier inventory)

Table 3.4: Timeline of currently available and future (Landsat 8, Sentinel 2) optical satellite data with at least one band in the SWIR of at least 30 m spatial resolution. The change in the colour for ETM+ indicates the scan-line-corrector failure in 2003.

3.1.2 Data availability

Landsat data

Neglecting the only rarely available Landsat 4 data from 1982 and 1983, data from Landsat 5 are available **since 1984** and represent the longest time series available for glacier mapping. This now 27-year time series from a single EO sensor is indeed the longest on record. The TM sensor is thus unique in providing fundamental climate data records (FCDRs) of the ever-changing conditions of the Earth's surface (see Table 3.4). Due to the commercial distribution of Landsat data for a limited period, data availability was limited in the past. Since the opening of the archive at USGS in 2008, the situation completely changed. In regard to global glacier mapping, the Geocover dataset from the Global Landcover Facility GLCF (Tucker et al., 2004) provided an early first glimpse of potential future assessments (e.g. Citterio et al., 2009). The real breakthrough came in 2010 with the general availability of L1T corrected (i.e. correctly orthorectified) scenes. These scenes now also fit to other geospatial datasets (e.g. DEMs) and can be properly digitally combined. However, some care is required in regions of DEM artefacts (e.g. the voids in the SRTM DEM) were locally the orthorectification is much less precise and the digital combination of different datasets challenging.

For product generation in the selected key regions only suitable scenes can be used. Suitable in this regard means **without clouds** and acquired at the **end of the ablation period** without seasonal snow outside of glaciers. This is the first and most important criterium for a scene to be selected from an archive. Considering the 16-day revisit period, these constraints are difficult to achieve each year for most mountain regions and often more than 5 years passed before the next suitable scene was acquired. Though this is still acceptable for the typical repeat period of glacier inventories (a few decades), it could take much longer than 5 years (e.g. 22 years for the Jostedalsbreen in Norway). Rather often, clouds hide a larger part of a scene which is otherwise perfect. In this case it is convenient to only process the cloud-free part of the scene and add the remaining glaciers from another scene (in case of overlap) or another date. The automatic cloud cover assessment is of no help in this regard to pre-select suitable scenes, as it is important where the clouds are located. For example, in autumn scenes, morning fog often covers large parts of a scene without hiding any glacier. This implies that all suitable scenes have to be found by visual inspection.

Though scenes with adverse **snow conditions** have been and are still used to delineate glaciers, this cannot be recommended. It is always preferable to wait for a better scene than to map glaciers under seasonal snow cover. Indeed, a glacier surface is characterized by being much smoother than the surrounding terrain and a well-trained analyst might be able to track the glacier boundary correctly even when covered by seasonal snow. However, this applies more to the 1 m pixel scale (aerial photography, high resolution satellite imagery) than to 15 m ASTER or 30 m Landsat pixels. For these sensors the huge archive of scenes should be utilized to find the most appropriate one. So the criterion of a close temporal coincidence of all scenes used to create a glacier inventory in a specific region is much more relaxed than the seasonal snow issue. An acquisition period of a few years is unproblematic, but it needs to be properly traced.

Coming to the scenes available in the USGS archive, the **receiving station** plays a certain role for data availability. The USGS archive does contain also scenes from other (non-US) receiving stations, but not from all. For example, the European archives from Fucino and Kiruna (glaciers from the Alps, Scandinavia and Svalbard) are only partly included. A large number of suitable scenes is thus missing and it is required to carefully analyse the entire archive. A special point to consider when browsing through the available scenes in glovis, are the different collections (see http://glovis.usgs.gov/AboutBrowse.shtml). In specific cases a scene that is not available in the standard archive can be found in one of the other collections, e.g. in the various Global Land Surveys (GLS). They are always worth a look.

The **temporal coverage** for a specific region is highly variable from scene to scene. This depends not only on the receiving station or the period with commercial distribution of the data (where images were acquired less frequently), but also on the cloud conditions and the programming of the respective sensor. As the onboard recording capability is limited, only a small part of an entire path can be recorded. As nearly each glacierized region has a specific path, the recording limitation does only apply for a few regions (e.g. Greenland vs. Patagonia, Canadian Arctic vs. Canadian Rockies). The temporal availability for a specific scene ranges from one scene every 16 days for the entire year and all years (only theoretically) to only a few scenes at all. The former conditions are found in some regions before 1990 and the latter in the decade before 2000, when Landsat data were commercially distributed. The situation of data availability improved for the period covered by the Landsat 7 ETM+ sensor (1999-2003) and deteriorated again afterwards.

During the normal phase operation of operation from the Landsat 7 ETM+ sensor (from 1999 to May 2003), only a few scenes from Landsat 5 are available. With the failure of the scan line corrector, Landsat 5 was brought back on line to complement Landsat 7 acquisitions. The Landsat 7 scenes with **scan line correction** (SLC) failure are still useful for glacier mapping if (i) the region of interest is in the centre of a scene where the influence of missing scan lines is small, or (ii) scenes can be mosaicked to fill the scan line gaps. In particular when snow conditions are similar, it is often the case that the striping is not at the same place, i.e. black values (DN=0) in one scene can be replaced with correct values from another scene. Of course, both scenes should be acquired within a few years (depending on the rate of glacier change) and the use of fused scenes should be properly documented in the meta data.

The points summarized above result in the following **procedure** for data processing. At first, a key region is identified (see Table 3 in the URD; Glaciers_cci, 2011a) and the responsible GLIMS regional center (RC) is contacted in regard to the status of the region. After clarification of the required action, a data processing need might be identified and the various data collections in the USGS archive are analysed. If potentially suitable scenes are identified, they are downloaded and snow conditions are analysed or compared among different scenes. If multiple scenes are suitable, the one closest to the year 2000 is selected (for best temporal coincidence with the acquisition date of the SRTM DEM) and processed. The glacier outlines are forwarded to the responsible RC for inspection and comments, before they are submitted to GLIMS. The path-row values of the Landsat scenes for the current list of key regions is given in Table 3.5. The exact dates of each scene will be determined shortly before data production.

Region	Path-Row	Region	Path-Row
Alaska: Brooks Range	70-11, 72 to 76 -12,	Chile/Argentina: TBD	TBD
Canada: Baffin Island	15,16-13,14; 17, 18, 19-13, 21-11; 24-10; 26-10; 28-9; 31-9	Islands: South Georgia New Zealand	206-98 75-90, 76-91
Greenland: West coast	16/18-8, 19-7, 23/26/ 29-6, 31/33-5, 35-3/4	Antarctic Peninsula:	215 to 219 - 104 to 108, TBD
Himalaya: Karakorum	147/148/149 - 35/36	Asia: TBD	TBD

Table 3.5: Landsat path and row numbers of the currently selected key regions for product generation. Due to the ongoing work, in some regions the scenes will only be determined before they are processed. They are indicated with TBD (to be determined).

ASTER data

The ASTER sensor on-board the Terra satellite flies in formation with Landsat 7, i.e. image acquisition since 1999 are performed at the same day. This allows us to perform comparative studies with the two sensors (e.g. Paul and Kääb, 2005) and, in principle, also to fill data gaps of ETM+ with ASTER data. However, ASTER scenes need to be orthorectified before and this requires to collect ground control points (GCPs) from topographic maps or, where available, from the orthorectified ETM+ panchromatic sensor (with 15 m resolution) and a DEM. Doing this for two ASTER scenes might take about a week which translates to about one person month of work to cover an entire Landsat scene. We will thus not do it in Glaciers_cci, but suggest that professional organisations or space agencies (e.g. JAXA and/or NASA) take care for this step, like it is already done for Landsat scenes by USGS.

ASTER image acquisitions over glaciers are a key element of GLIMS and data acquisition requests were especially designed for this target (Raup et al., 2000). This resulted in special low gain settings over glacierized regions to reduce detector saturation over snow. Though ASTER scenes had some problems in the beginning (with striping) and in the past (with SWIR detector cooling), the relevant bands for glacier mapping (ASTER 1-4) are still unaffected and provide excellent data. It is intended to use already orthorectified ASTER scenes for inventory creation in regions like Svalbard, where appropriate Landsat scenes are sparse and the required topographic information for proper orthorectification are already available. The other points mentioned above for Landsat also apply for ASTER.

3.1.3 Data access conditions

Landsat data

For the Landsat data from USGS the ordering and download via the http://glovis.usgs.gov website is very easy and straightforward. An alternative site (with a differing data search functionality) exists at http://earthexplorer.usgs.gov. The data are freely available and access is provided via a personal login with password. The free access (also in the future) is guaranteed (USGS, 2008). Due to technical development, the download portal changes through time (see http://glovis.usgs.gov/WhatsNew.shtml). We will not speculate here if these future changes will be positive or negative, but it is assumed that the possibility to give feedback via the USGS customer service will allow them to revise problematic changes. Other data browsing and download portals for Landsat data (e.g. from CCRS and ESA EOLI) are available as well, but they do only provide the raw data (system corrected but without orthorectification) and are more complicated to use.

ASTER data

Available ASTER scenes are also at best searched inhttp://glovis.usgs.gov. The ordering tool at https://wist.echo.nasa.gov/api/ is more difficult to use (text based search with multiple choice selectors for numerous other datasets) but works as well. When scene IDs are already known the access is more comfortable as it provides direct access to the data. However, ASTER scenes are (yet) only available in path orientation and the orthorectification has to be performed by the analyst. Data are freely available for registered GLIMS participants and the download is via ftp. The free access to ASTER data via GLIMS participation is currently guaranteed to the consortium until 2013.

SPOT data

Scenes from all SPOT sensors can be found through the Sirius catalogue of SPOTimage http://catalog.spotimage.com. The search facility produces a text file with attached quicklooks which are only visible after clicking and hence a rapid visual assessment is not possible. The size and quality of the quicklooks is also not as good as the quicklooks from the glovis browser and hence it is difficult to assess their value for glacier mapping before ordering data at original resolution. Due to a mutual agreement between ESA and SPOTimage (the company in charge of the commercial distribution) from 2006, data from the SPOT satellite can be ordered through the ESA portal http://eoli.esa.int. Within a limited overall number of scenes per year (10,000), data are available at no cost for an agreed CAT-1 proposal. As SPOT data might only be used occasionally in Glaciers_cci, the limitation on the number of scenes is not a problem. For the purpose of Glaciers_cci, some SPOT scenes are already available). SPOT scenes have in general to be orthorectified by the analyst, but the quality of the geolocation that can be achieved without GCPs is much better than for ASTER data.

Description	Landsat	ASTER	SPOT
Browser	glovis.usgs.gov	glovis.usgs.gov	catalog.spotimage.com
Order/download	glovis.usgs.gov	https://wist.echo.nasa.gov/api/	eoli.esa.int
Search via	path/row & map	path/row & map	map
Price	no cost	no cost for GLIMS participants	no cost from ESA (CAT-1)

Table 3.6: Summary of data access conditions for the core EO data that can be used for product generation. All data can be assessed via ftp after login.

3.2 EO data for product validation

3.2.1 Data sources

Two types of validation will be performed for the glacier area product: (**A**) internal validation with the same satellite scene as used for product generation (each individual product), and (**B**) external validation using higher-resolution datasets for specific test sites and a few selected glaciers. The type (A) validation is required as the algorithm applied for the automated classification of glaciers has omission (ice with debris cover or in shadow, clouds) and commission (lakes, vegetation, ice clouds) errors. Though it is one aim of the project to further improve the automated part of the classification, the most efficient and accurate way to correct wrongly classified regions is manual editing according to visual inspection. This process is based on the overlay of vector outlines on contrast enhanced composite images with bands 3, 2, and 1 (as RGB), 4, 3, 2 and 5, 4, 3 (see Table 3.2). Whereas the former is particularly useful for correctly identifying ice and snow in cast shadow, the latter is used for correcting all other errors. So the standard processing sequence does already include the removal of wrongly classified objects and an adjustment of the glacier outline to a 'ground truth' (i.e. the satellite image). Assuming that the analyst correctly identifies and corrects all wrong classifications, each glacier area product is already validated. In the case of a wrong or missed correction by the analyst, there is a potential for later correction once the outlines are available in the GLIMS database for inspection by others.

Product validation of type (B) is more difficult due to several constraints that need to be considered. The first point is that glaciers are rapidly changing objects. This refers to the glacier front on an annual time scale, as well as to snow conditions on a daily to weekly temporal scale (depending on the sensor resolution). As snow in mountain regions has the tendency to accumulate along the boundary of a glacier (e.g. avalanche deposits), only high-resolution EO data that have been acquired in the same week (or under identical snow conditions) can be used for product validation. This constraint can cause a problem with aerial photography from national surveys that need to be acquired at high solar elevations (e.g. during August) with related adverse snow conditions for glacier mapping (see Paul and Andreassen, 2009). Such high resolution EO data (or the vector data generated from them) cannot therefore be used for validation, i.e. good **temporal** agreement is a major constraint.

Assuming that temporarily suitable high-resolution EO data for validation could be found, the next important issue is spectral agreement. This is, however, never found on an operational base as none of the available EO sensors or digital cameras has a TM band 5 equivalent SWIR sensor. At best, a NIR band is available that might provide improved contrast over snow and along the bare ice/rock boundary. Identification of clouds is nearly impossible with both panchromatic and NIR images. The consequence of the missing SWIR band is that ice and snow can be interpreted differently and the resulting outlines or glacier extents are no longer usable as a 'ground truth' for validation. So when classifying glaciers from different **spectral** bands, differences in the interpretation are unavoidable.

A final point to be considered is **spatial** resolution. Though it is generally assumed in the scientific literature that higher resolution automatically gives better visibility and quality, this is actually not the case for several reasons. For natural objects like glaciers, higher resolution means that other features become visible. Given that the optical contrast is good and both data sets are from the same date, a close-up is always also a close-up of the problematic regions and the boundary of a debris-covered glacier is not necessarily better discriminated at 0.5 or 1 m resolution (see Fig. 1 in the PSD; Glaciers_cci, 2011b). In general, only the number of pixels that need a decision is increased and new problematic features become obvious (e.g. dead ice in a connected lateral moraine). For validation purposes it is thus beneficial to only consider glaciers with good optical contrast of the boundary in the high-resolution image.

Apart from the technical points mentioned above, there are also **methodological issues** that need to be considered. As Paul et al. (2003) had shown, the size of a glacier does also depend on the spatial resolution. When a vector outline of a glacier (e.g. as digitized from aerial photography with 1 m spatial resolution) is resampled to a different cell size, the area enclosed by the line changes. So when the glacier size with 1 m pixels is directly compared with the 30 m pixel size value, a resampling induced difference is included that is not related to product accuracy. Hence, the glacier outline derived from a high-resolution sensor must first be resampled to the resolution of the respective satellite-derived outline and the area value can then be compared. Of course, the other critical issues mentioned above (e.g. seasonal snow) need to be considered as well for such a comparison (see Fig. 3.1).

The difficulties in finding a technically appropriate 'ground truth' for product validation have two consequences:
(a) we propose alternatives for product validation and error assessment to the normally applied high-resolution sensor comparison (more details will be provided in the PVP; Glaciers_cci, in prep.), and
(b) we cannot yet exactly specify (path, row, date, sensor) the data sets that will be used for product validation.

However, based on previous studies we provide in Table 3.7 an overview of the characteristics of potentially suitable sensors for type (B) validation. A sufficient number of scenes in various regions of the world (see selected regions in 2.1.1) are available and will be provided in the PVP (Glaciers_cci, in prep.).

Characteristic	Kompsat 2	Quickbird	Ikonos 2	Cartosat 1	GeoEye	WorldView
Launch	2006	2000	1999	2005	2008	2007
Resolution (pan/ms)	1/4	0.66/2.44	0.8/3.3	-/2.5	0.5 (pan)	0.5
Swath width [km]	15	16.5	11	30	15	16.4
Repeat cycle [days]	14	3-4	2-3	5	3-3	2-3
Accuracy w/o GCPs		20	10		2	6

Table 3.7: Basic characteristics of the high-resolution sensors that are suitable for product validation. Several scenes from these sensors are available through Google Earth™. Sources:
http://www.spatialenergy.com/products_imagery.html
http:// database.eohandbook.com/database/missionindex.aspx

In addition to these high-resolution but space-based sensors, there is also the potential to use **aerial photography**. Here the major constraints are the huge number of available images, the generally missing browsing capability and orthorectification, the restricted (national) access with high costs for small regions, and the often inappropriate time of acquisition in regard to snow conditions. However, there are three potential solutions for including such aerial photography in product validation: (i) through special access conditions for national imagery, (ii) by validation activities performed by CRG members, and (iii) by using screen shots from images available in Google Earth™. The latter will also be applied by the Glaciers_cci project, as these images fulfil nearly all of the criteria listed above, i.e. they are already orthorectified, have a time stamp, are browsable, globally and freely available, come with up to 0.5 m resolution, and have at least sometimes perfect snow conditions. However, the geocoding information (pixel size and upper left corner) needs to be determined by iterative adjustment. As the quality of this iterative geocoding might not be visible in comparison to 30 m Landsat data, we will also compare it against original high-resolution satellite data and aerial photography.

3.2.2 Data availability

As mentioned above, product validation will be based on (A) the satellite image as used for generating the glacier outlines and (B) on higher resolution data sets. As we have decided to perform product validation only in regions where such data sets are available, there is no problem in regard to data availability. In Table 3.8 we provide a first overview on the selected regions for product validation and the available data sets from the high-resolution sensors. Most of these data sets refer to the 2000-2010 period. In total about 60 glaciers can be used for product validation. Further details will be provided in the PVP (Glaciers_cci, in prep.).

Region	Landsat	HR sensor	Glaciers
Alaska	68/69-17	Ikonos	10
Greenland	224-10	Quickbird	5
Norway	201-17	Aerial	10
Alps	193-27	Aerial	5
	193-27	Ikonos	10
	192-27	Quickbird	10
Himalaya	140-41	Kartosat	5

Table 3.8: Selected regions for product validation with Landsat path-row specification, applied high-resolution (HR) sensors and number of suitable glaciers in each HR scene.

3.2.3 Data access conditions

For type (A) validation the data access conditions are described in section 3.1.3. For type (B) validation, there are basically four options: those listed at the end of section 3.2.1 under points (i) to (iii) for aerial photography, and (iv) data procurement of high-resolution data acquired by the satellites listed in Table 3.6 (e.g. via http://www.npoc.ch). The data access conditions for each of the satellites are subject to frequent and sudden change (e.g. promotional offers). Before specific scenes are ordered from the national or international distributor, it will be analysed if suitable scenes are also available in Google Earth™. These are already orthorectified and match rather well to the L1T Landsat data (Fig. 2.1). However, the geometrical fit needs to be assessed on a case-by-case basis. Some national mapping authorities (e.g. Statens Kartverk in Norway) provide free high-resolution aerial photography as geocoded jpg files also online (http://norgeibilder.no). For images with suitable snow conditions, we will use these data for product validation. Moreover, consortium partners have free access to aerial photography from national mapping authorities due to special agreements (GIUZ: Switzerland, Enveo: Austria, GUIO: Norway and Svalbard).

For the data sources described above, data access is via ftp, screen shot or image export from the webpage. Apart from the validation activities performed by the CRG and otherwise freely available datasets, validation data used by the consortium cannot be shared.

3.3 Auxiliary data for product generation

3.3.1 Data sources

As mentioned in section 3.1.1, a mandatory data set for creation of the glacier inventory product is a DEM. For global scale applications, also the DEM has to fulfil a number of constraints: It must be globally available, generated in a consistent way, and fit to the satellite data in a spatial and temporal sense. With the USGS L1T Landsat TM/ETM+ data being used as the main source for product generation, the GLS2000 DEM that is also used for the orthorectification of the Landsat scenes would be the most suitable dataset. However, this dataset is a compilation of DEMs from different sources, including the SRTM DEM (in the version from CGIAR), National Elevation Datasets (NED), the Canadian Digital Elevation Dataset (CDED), Digital Terrain Elevation Data (DTED) from various countries, and the GTOPO 30 DEM (USGS, online: http://www.glcf.umd.edu/data/glsdem). It can be downloaded from ftp://ftp.glcf.umd.edu/glcf/GLSDEM/.

Over large regions the GLS2000 DEM is based on the void-filled SRTM DEM from CGIAR. As this version has locally strong artifacts (in the former SRTM data voids) as a study by Frey et al. (subm.) has shown, these elevation errors are transferred to the orthorectification and result in a shift of the geolocation by up to five pixels (150 m) or more. In consequence, while the GLS2000 DEM fits (spatially) to the Landsat-derived glacier outlines, it contains wrong elevation values in the data voids and thus the topographic inventory parameters would have large errors. Our current strategy is to compare the SRTM DEM with the ASTER GDEM and then decide which of the DEMs will be used for a specific purpose. The advantage over the GLS2000 DEM is the better traceability of the data source. Characteristics of the DEMs to be used for product generation are summarized in Table 3.9. With the release of the new ASTER GDEM2, the number of artifacts in this DEM might be considerably reduced and the former GDEM will no longer be used.

Description	SRTM	CGIAR DEM	GDEM
Weblink	http://srtm.usgs.gov	http://www.cgiar-csi.org/	http://www.ersdac.or.jp/GDEM/E/2.html
download	http://dds.cr.usgs.gov/srtm/version2_1/SRTM3	http://srtm.csi.cgiar.org/selection/inputCoord.asp	http://www.gdem.aster.ersdac.or.jp/
Reference	Farr et al. (2007)	Reuter et al. (2007)	Hayakawa et al. (2008)
Format	1 by 1 deg tiles	5 by 5 deg tiles	1 by 1 deg tiles
Data Type	Raster (.bil)	Raster (.bil)	Raster (.bil)
Projection	geographic	geographic	geographic
Coverage	57 S to 60 N	57 S to 60 N	83 S to 83 N
Sensor	microwave	SRTM + maps	optical
Technique	interferometric	mosaiced	photogrammetric
Sources	Space Shuttle mission STS99	SRTM & interpolation	ASTER optical stereo
Resolution	3” (ca. 90 m)	3” (ca. 90 m)	1” (ca. 30 m)
Time stamp	Feb 2000	Feb 2000	2000-2007
Problems	Data voids	interpolation errors	local artifacts
Remarks	A globally complete version with 30” resolution is also available	Voids in the SRTM DEM were filled with ancillary data	The GDEM validation summary report is available from various sources

Table 3.9: Main characteristics of the DEMs used for product generation.

As the SRTM DEM is only available south of 60° N, it can thus not be used for all glaciers and icecaps (e.g. in the Canadian and Russian Arctic). The auxiliary DEMs used for product generation thus include further DEMs such as the NED, CDED and DTED. The particular disadvantage of the latter datasets is their historic date (most of them originate in the 1950s to 1980s) and the often unknown date of acquisition. The best access to national DTEDs is from the viewfinderpanoramas.org website. The characteristics of all three data sources are compiled in Table 3.10.

Description	NED	CDED	viewfinder
Download	http://seamless.usgs.gov/ned1.php	http://www.geobase.ca/geobase/en/data/cded/	http://www.viewfinderpanoramas.org/dem3.html
Reference	USGS	Canadian Council on Geomatics	Jonathan de Ferranti
Format	seamless	map sheets	1 by 1 deg tiles
Data Type	Raster (.bil)	Raster (.bil)	Raster (.bil)
Coverage	USA	Canada	global
Sensor	aerial	aerial	various
Technique	digitization and interpolation	digitization and interpolation	photogrammetric
Sources	topographic Maps	topographic maps	public, maps, other
Resolution	1” (30 m), Alaska: 2“	1:50000 & 1:250000 maps	various
Time stamp	before 1970	around 1985	various
Shortcomings	interpolation artifacts	not complete at 1:50’000	local gaps

Table 3.10: Main characteristics of additional DEMs for product generation.

3.3.2 Data availability

All DEMs listed above are freely available, the covered period and regions are listed in Tables 3.9 and 3.10. While the most suitable data set is the GLS2000 DEM as used for the orthorectification of the Landsat scenes, this DEM is in general not publically available and mosaicked from various sources that are difficult to identify. In this regard preference is given to the original data sources as listed in the two tables above. There is also a clear preference for the SRTM DEM for the inventory parameters and the drainage divides (as this is the globally most accurate and consistent data set), but comparison with other available DEMs can always reveal more suitable (or accurate) DEMs from the listed alternative sources (e.g. when the time stamp is less important) for a specific purpose. Of course, outside the SRTM coverage these DEMs have to be used. The required data quantity will depend on the number of satellite scenes processed and the data source (e.g. 1 by 1 vs. 5 by 5 degree tiles). As all data are freely available, the exact number of downloaded DEM tiles does not really matter. When a mosaic is created from several tiles, it is recommended to first mosaic all tiles (in geographic coordinates) and reproject the mosaic afterwards.

3.3.3 Data access conditions

All DEMs can be downloaded for free via ftp from the web addresses given above and in the PSD. The GDEM requires a login and password. Weblinks for download are given for all DEMs in Tables 3.9 and 3.10.

3.4 Auxiliary data for product validation

Vector outlines from glaciers and icecaps derived from aerial photography are available for many countries (e.g. Canada, Greenland, Norway, Austria, Switzerland). In principle, these data sets could be used as an independent validation source. However, all of these datasets have shortcomings: they have been acquired under adverse snow conditions, the mapping date is not reported, or the analysts were cartographers rather than glaciologists (which often results in the inclusion of seasonal snow). For this reason we will use these data sets only to aid in product generation rather than validation. For validation we will only use quality controlled (e.g. acquisition date available, snow conditions appropriate) original data sets that were transformed to vector outlines by members of the CRG or the EO team of the consortium. The often occurring differences in the interpretation of glacier extents by other analysts will be revealed in the round robin. As an example to justify this decision, we show in Fig. 3.1 a comparison of Landsat derived glacier outlines from 2003 (yellow) with the outlines in the Austrian glacier inventory (black) that was derived from aerial photography acquired between 1997 and 1999 (Lambrecht and Kuhn, 2007). Due to the adverse snow conditions in some of these photographs (indicated by the 'nervous' shape of the outlines), seasonal snow was likely mapped as glaciers and too large glacier sizes resulted.

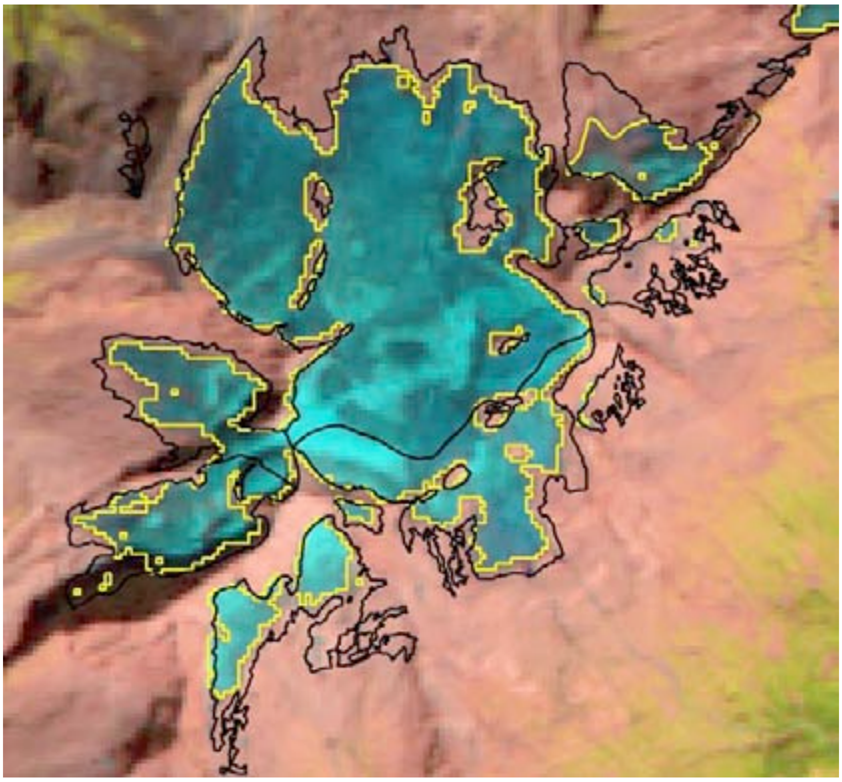

Fig. 3.1: Comparison of glacier outlines around Olperer Ferner in the Zillertal Alps (Austria) derived from a Landsat TM scene of 2003 (shown as a band 543 composite in the background) in yellow with the extents mapped for the Austrian glacier inventory in 1998 (black). A small difference in projection is also visible. Image width is 5 km, north is at top.

4. Elevation change

4.1 EO data for product generation

4.1.1 Data sources

The elevation change products are based on (1) DEM differences and (2) altimeter-derived point elevation differences (using the repeat-track and/or cross-over methods). The DEM difference product will mainly rely on ASTER DEMs, SRTM, SPOT5 HRS SPIRIT, and where available on national DEMs combined with ICESat GLAS elevations for georeference.

ASTER DEMs

These data will be used directly as provided from the USGS NASA LP DAAC through NASA WIST as AST14DMO on demand product. The DEM of this product has a spatial resolution of 30 m over 60 by 60 km and a vertical accuracy of roughly 15 m for suitable surface conditions (e.g. Hirano et al., 2003; Kääb, 2002). The product comes with orthoprojected satellite image bands. Comparison of the band 3N (nadir) and 3B (back-looking) orthoimages provides a qualitative assessment of the underlying DEM since DEM errors will be visible as shifts between the orthoimages (Kääb, 2008). However, because AST14DMO relies only on on-board satellite position and attitude angles for forward intersection of terrain elevations, and no GCPs, the absolute (horizontal) accuracy of the entire DEM can be on the order of 50-100 m or worse (ASTER pointing accuracy; Nuth and Kääb, 2011). This offset can be quantified and corrected by co-registration to a second DEM or to ICESat GLAS elevations.

SPOT5 HRS SPIRIT

For selected polar regions DEMs from SPOT5 high resolution stereo are available as compiled during the SPIRIT programme. SPOT5 HRS consists of a forward looking and a backward looking channel. The resulting stereo DEMs were produced by the French mapping agency and have a reported uncertainty of 10–25 m vertically and greater than 15 m in the horizontal plane (Korona et al., 2009). Though small, this offset can be quantified and corrected by co-registration to ICESat GLAS elevations or more accurate DEMs.

SRTM DEM

The Shuttle Radar Topography Mission (SRTM), launched in February 2000, mapped the Earth from 60° N to 56° S using single-pass synthetic aperture radar (SAR) interferometry. SAR interferometry uses the phase differences between two radar images acquired with a small base-to-height ratio. These phase differences are the photogrammetric equivalent to a "parallax" measurement allowing retrieval of topography. We will use the SRTM 3" V2 dataset without void filling for this purpose. A number of glacier elevation change studies have used this as a base dataset to compare to both newer and older data products. Typically reported vertical uncertainties of the dataset are ±10 m, which (e.g. Rodriguez et al., 2006) is lower than the mission objectives of ±16 m (Farr et al., 2007). However, vertical biases are present due to instability of the sensor and/or platform, and elevation-dependent biases have also been shown due to penetration of the C-band radar waves (centre frequency at 5.3 GHz) into snow and ice of 1 to 10 m depending upon the snow conditions (i.e. dry versus wet) in Greenland and Alaska (Rignot et al., 2001). In Svalbard, the volumetric phase centre of the C-band varied from 1 to 5m along a profile from ablation to firn zones, respectively. Corrections for depth penetration are rarely used for the SRTM data and it is very difficult to correct them as knowledge of the snow conditions at the time of acquisition is required but generally unavailable.

National DEMs

National DEMs have been generated in many countries from photogrammetric techniques applied to aerial photography, in most cases as a base for topographic maps. These DEMs often come with national restrictions for redistribution and can be rather expensive for small regions covered (also depending on the acquisition technique and accuracy or spatial resolution of the DEM). For this reason such data sets will only be applied in Glaciers_cci when they are freely available and of sufficient quality (as visual inspection of hillshades will reveal), for example the CDED of Canada or DED from Alaska (Le Bris et al., 2011). Several of these DEMs were acquired in the mid-1980s, so compared to the SRTM DEM or other DEMs they provide already a valuable source for calculation of elevation changes (e.g. Schiefer et al., 2007; Paul and Haeberli, 2008). As for all DEMs derived from optical data, the accuracy in the accumulation region or in shadowed terrain is reduced due to lacking optical contrast. From this perspective DEMs derived from LIDAR (scanning) are much more precise in these regions (e.g. Abermann et al., 2010). As LIDAR are much less widely available and even more expensive than the normal national DEMs, DEMs from LIDAR data will be used in Glaciers_cci only for validation purposes.

ICESat GLAS Altimetry data

In 2003, the NASA Ice, Cloud, and land Elevation Satellite (ICESat) was launched with the Geoscience Laser Altimeter System (GLAS) acquiring elevation measurements in a 40-70 m elliptical footprint every 170 m in along-track direction. The cross track resolution was determined by the 91 day ground track repeat cycle which yielded 90 km track spacing at the equator and 15 km at 80 degrees latitude. With three lasers on board, only one operating at any given time, ICESat obtained global coverage of elevations along profiles with a denser track sampling in high latitudes due to the polar orbit. The inclination of 94° resulted in latitude coverage to 86° north and south of the equator. The rapid failure of the first laser invoked a curtailed orbital acquisition program. Nonetheless, the GLAS lasers operated for the following five years, collecting nearly two billion elevation point measurements before the last laser failed in November 2009.

The altimeter has proven to be accurate to approximately one decimetre over flat deserts (Fricker et al., 2005) and ice sheets (Shuman et al., 2006), and crossover track differences over low-sloped large glaciers show an accuracy of the order of approximately half to one metre (Brenner et al., 2007; Moholdt et al., 2010). ICESat has been extremely successful for glacier applications in terms of elevation changes but also for determining the accuracy of newer satellite products and older topographic maps. The 1B level product, GLA06, is available for smooth ice sheets, whereas the level 2 product, GLA14, is available for rougher terrain surface. The products vary by the number of Gaussian peak fits used to determine the maximum return-echo amplitude, maximum 2 and 6 respectively. The mean difference between the two products is -0.15 m though variations of up to ±3m occur. For the Glaciers_cci project the most recent release will be used, currently #31, that is freely accessible through the NSIDC website (http://nsidc.org/data/icesat). Table 4.1 summarises the release schedule. It is ordered by release date, with the most recently received campaign listed first.

Beginning with Release-28, an YXX pattern for release numbers is used in file names. The release-31 products have an YXX release number of 531. The Y portion (known as the Y-code) of this new three-digit naming convention ensures that similar Precision Orbit Determination (POD) and Precision Attitude Determination (PAD) procedures are completed for similarly-named elevation data products. The Y-code in the YXX release number indicates the calibration level; the higher the Y-code, the higher the level. This change mostly concerns products GLA06 and GLA12-15. Although present in other file names, the Y-code is not relevant for other data, as the POD and PAD only affect the geolocation of the laser spot. Elevation data from different campaigns having the same Y-code may not necessarily have the same elevation quality (due to spacecraft instrumentation, orientation, and other factors), but generally a similar quality http://nsidc.org/data/icesat/yxx_release_numbers.html

Temporal Coverage (dd-mm-yyyy)	Laser Identifier	Orbit	Release Date (dd-mm-yyyy)
30-09-2009 to 11-10-2009	2F	91-day	28-05-2010
09-03-2009 to 11-04-2009	2E	91-day	27-05-2010
25-11-2008 to 17-12-2008	2D	91-day	24-05-2010
20-02-2003 to 21-03-2003	1A	8-day	18-05-2010
21-03-2003 to 29-03-2003	1B	8-day	18-05-2010
18-05-2004 to 21-06-2004	2C	91-day	12-05-2010
17-02-2004 to 21-03-2004	2B	91-day	05-05-2010
04-10-2003 to 19-11-2003	2A	91-day	30-04-2010
25-09-2003 to 04-10-2003	2A	8-day	30-04-2010
04-10-2008 to 19-10-2008	3K	91-day	27-04-2010
17-02-2008 to 21-03-2008	3J	91-day	21-04-2010
02-10-2007 to 05-11-2007	3I	91-day	25-03-2010
12-03-2007 to 14-04-2007	3H	91-day	22-02-2010
03-10-2004 to 08-11-2004	3A	91-day	21-01-2010
17-02-2005 to 24-03-2005	3B	91-day	07-01-2010
20-05-2005 to 23-06-2005	3C	91-day	14-12-2009
21-10-2005 to 24-11-2005	3D	91-day	01-12-2009
22-02-2006 to 28-03-2006	3E	91-day	17-11-2009
24-05-2006 to 26-06-2006	3F	91-day	03-11-2009
25-10-2006 to 27-11-2006	3G	91-day	19-10-2009

Table 4.1: GLAS data current release schedule for GLA06, GLA12, GLA14.

ERS-1

ERS-1, launched by ESA in July 1991 (Remy and Parouty, 2009; Rosmorduc et al., 2011), was the first polar-orbiting satellite with an inclination of 98.5º which carried a radar altimeter on-board. The satellite had a standard orbit repeat cycle of 35 days leading to a cross-track sampling of 15 km at a latitude of 70º. Two other repeat cycles of 3 days and 168 days have been operated for calibration purposes, for the observation of specific ice zones and for the mapping of the geoid (see Table 4.2). This allowed a dense sampling of ice areas. The radar altimeter operated at Ku band (13.8 GHz) with a pointing nadir acquisition and collected data continuously and homogeneously until May 1996 covering the latitudes from 82º N to 82º S. The measurements were carried out at a 0.05 s^{-1} frequency which corresponded to a 350 m spatial resolution along the satellite track. The footprint varied from 16 to 20 km. In ocean mode a chirped pulse of 20 micro-second duration was generated with a band width of 330 Mhz which corresponded to a range resolution of about half a metre (0.45 m) (Rosmorduc et al. 2003). However, the range measurement performance over the ocean was about one order of magnitude greater (4.5 cm). This was achieved by fitting the shape of the sampled echo waveform to a model function, which represents the form of the echo. For tracking in ice mode an increased dynamic range was used, obtained by reducing the chirp bandwidth by a factor of four to 82.5 MHz, resulting in a coarser resolution of 2 m.

Temporal Coverage (dd-mm-yyyy)	Orbit	Phase	Notes
25-07-1991 to 10-12-1991	3-day	Commissioning phase	Observations of the calibration sites
28-12-1991 to 31-03-1992	3-day	Ice phase 1	Observations of specific ice zones
02-04-1992 to 14-04-1992	3-day	roll tilt mode	Different SAR incidence angle observations
14-04-1992 to 23-12-1993	35-day	Multidisciplinary phase 1	Observations for applications of land/ice mapping with the SAR
23-12-1993 to 10-04-1994	3-day	Ice phase 2	Repeatition of the obsevations of ice phase 1, after a two year period
10-04-1994 to 27-09-1994	168-day	Geodetic phase 1	Observations for mapping the geoid
28-09-1994 to 21-03-1995	168-day	Geodetic phase 2	Observations for mapping the geoid
21-03-1995 to 02-06-1996	35-day (ultimate orbit)	Multidisciplinary phase 2	Multidiciplinary mission observations and cross-calibration with ERS-2

Table 4.2: Overview of the different operation phases of ERS-1.
Source: http://earth.esa.int/ers/eeo/ERS1.1.7.html

ERS-2
The ERS-2 satellite was launched on April 1995 to ensure the continuation of ERS-1 data provision and it carried a similar radar altimeter. For twelve months in 1995-1996, during the Tandem mission, ERS-1 and ERS-2 were operated in the same 35 day repeat orbit, one day apart with all instruments simultaneously operating. Since June 1996 ERS-2 has been the primary operating satellite with ERS-I maintained as back-up and for occasional tandem campaigns. In June 2003, the onboard tape recorder of ERS-2 used for the altimeter data experienced a number of failures. This means that altimeter data were unavailable except for when the satellite was within visibility of ESAs ground stations over Europe, the North Atlantic, the Arctic and western North America. In July 2011, ERS-2 has been put out of service by bringing it down to a lower orbit. Characteristic properties of the radar altimeter are summarized in Table 4.3.

Property	Value
Emitted frequency (GHz)	Single-frequency (Ku) - 13.8
Pulse repetition frequency (Hz)	1020
Pulse duration (microseconds)	20
Bandwidth (MHz)	330 and 82.5
Antenna diameter (m)	1.2
Antenna beanwidth (degrees)	1.3
Specific features	2 bandwidths for ocean and ice measurements

Table 4.3: Technical data of the ERS-1 and ERS-2 radar altimeters (Rosmorduc et al., 2011).

Envisat RA-2
Launched in March 2002 by ESA, Envisat is the follow-on to ERS-1 and ERS-2. From the start of mission until 22 Oct 2010, Envisat operated in a 35-day repeat cycle orbit with a high inclination of 98°, like ERS-2 and some of the ERS-1 phases. On 22 October 2010, the orbit of Envisat was lowered to ensure an additional 3 years lifespan. After these orbit manoeuvres, the ground track changed and consequently the repeat cycle is now of 30 days. The Radar Altimeter 2 (RA-2) on board is a nadir-looking pulse-limited radar altimeter, is based on the heritage of the ERS-1 and ERS-2 radar altimeters. The RA-2 utilises a main nominal

frequency of 13.575 GHz (Ku-band) to measure the elevation of the ground surface (see Table 4.4). In addition to the Ku-band channel, the RA-2 had a 3.2 GHz (S-band) channel for the compensation of the delay caused by the ionospheric electron density. The S-band channel of RA-2 stopped working on 17 Jan 2008 and ionospheric corrections have since been based on models (ESA, 2008).

Property	Value
Emitted frequency (GHz)	Dual-frequency (Ku, S) - 13.575 and 3.2
Pulse repetition frequency (Hz)	1795 (Ku), 449 (S)
Pulse duration (microseconds)	20
Bandwidth (MHz)	320, 80 and 20 (Ku) - 160 (S)
Antenna diameter (m)	1.2
Antenna beanwidth (degrees)	1.29 (Ku), 5.5 (S)
Specific features	Dual-frequency for ionospheric correction, 3 bandwidths in Ku-band

Table 4.4: Technical data of Envisat RA-2 radar altimeter (Rosmorduc et al., 2011).

All previous satellite radar altimeters suffered data dropouts over areas with difficult terrain. To tackle this problem, RA-2 has a different tracker philosophy (Roca et al., 2009). The surface tracking system of the RA-2 is designed to be more robust than its predecessors, comprising an onboard autonomous resolution selection logic (RSL) (Resti et al., 1999a). Over rough terrain (coastal zones, land and ice), where data dropouts might occur, RSL changes the instrument into a coarser resolution mode (Resti et al., 1999a). Legresy et al. (2005) showed that the RSL extends the use of RA-2 to areas where past altimeters have failed. In Table 4.5 the suitable active sensors for glacier elevation retrieval available since 1991 with the main characteristics of the instruments are listed.

Satellite	Agency	Sensor	Repeat-cycle	Vertical resolution	Horizontal resolution (along track)	Vertical Accuracy (single pulse)	Availability
ERS-1	ESA	RA ku-Band 13.8 GHz.	35 days, 3 days, 168 days for some periods, covering limited regions	0.5 m on ocean surfaces 2 m on smooth and flat ice terrain	350 m	5 cm on ocean surfaces	1991-1996
ERS-2	ESA	RA ku-Band 13.8 GHz	35 days, 3 days for selected periods, covering limited regions	0.5 m on ocean surfaces 2 m on smooth and flat ice terrain	350 m	5 cm on ocean surfaces 2.5 m on ice with slope < 1°	1995-2011
ENVISAT	ESA	RA-2 Ku-Band 13.575 GHz	35 days 30 days from 22.10. 2010	0.5 m on ocean surfaces 2 m on smooth and flat ice terrain	390 m	2 m on ice with slope < 1°	2002-at present
ICESat	NASA	GLAS 1064-nm (near-infrared)	91 days (8 days during the Cal/Val phase)	15 cm	170 m	15 cm on flat terrain 10 cm on terrain with slope < 3°	2003-2009

Table 4.5: Overview of radar and laser altimeters applied for glacier elevation retrivial.

4.1.2 Data availability

ASTER data and DEM products are available globally, ongoing from 2000 on, though with individually varying cloud cover and suitability for DEM matching due to acquisition conditions (snow, sensor saturation). Generally, however, the total lack of suitable images over a given area is a rare exception. ASTER data availability under glovis.usgs.gov. (See also 4.1.2).

The SRTM covered the Earth surface between 60° N and 56° S during February 2000. Several original and void filled versions are available. For the elevation change product only the versions without void fills are suitable. Voids occur in mountains, and may hamper elevation change production over individual glaciers, but less on regional scales. (See also 4.3).

SPOT5 HRS SPIRIT DEMs are only available over selected polar glacier regions. Of main interest for the Glaciers_cci project is Svalbard that is nearly completely covered by data from the mid 2000s. The SPOT5 HRS SPIRIT DEM is available from:
http://polardali.spotimage.fr:8092/IPY/dalisearch.aspx.

National DEMs are available for free from several glacierized regions in the world including Canada and Alaska. In other regions the consortium has access to such data and can use it for product generation (e.g. Norway, Switzerland, Austria, parts of Italy). Rather often, these data sets refer to the mid-1980s or earlier implying that there are well suited for calculation of elevation changes (e.g. Berthier et al. 2010), but less suitable to derive topographic inventory parameters (e.g. LeBris et al., 2011).

ICESat GLAS foot prints cover the Earth from 2003-2009 along profiles with a maximum cross-track distance of roughly 50 km at the equator, between 40 and a few km for the glacier regions of interest for the Glaciers_cci. This distance between profiles makes elevation changes only possible for regional scales or large glaciers and ice caps. (See also 5.1.1).

ERS-1 provided continuously and homogenously acquisitions from its launch in July 1991 to May 1996, when ERS-2 radar altimeter was already operating. Indeed, from July 1995 to July 1996, ERS-1 and ERS-2 were operated in a Tandem configuration with all instruments simultaneously operating (see also 5.1.2). ERS-2 has been shut down recently, on July 2011, however in June 2003, the ERS-2 onboard tape recorder used for the altimeter data has experienced a number of failures. As consequence altimeter data were unavailable except for when the satellite was within visibility of ESA's ground stations. ENVISAT RA-2 data availability are available globally ongoing from March 2002.

4.1.3 Data access

ASTER data and products are freely accessible to registered users (Glaciers_cci: GUIO and GIUZ), best searched under http://glovis.usgs.gov and ordered through the website https://wist.echo.nasa.gov/api/. After ordering, the products are generated on demand and available after some hours to days, depending on the data quantity and work load of the processing unit. For the elevation change product, the ASTER product AST14DMO will be used (https://lpdaac.usgs.gov/lpdaac/products/aster_products_table). Note, that other documents available are outdated in terms of the DEM product.

Original SRTM data (i.e. without void fills) are freely downloadable from http://dds.cr.usgs.gov/srtm. A void-filled version of this DEM is downloadable from the website http://srtm.csi.cgiar.org. Thereby, the void mask are indicated by an additional mask, so that the CGIAR version can in principle be also used as original SRTM. However, tests by the consortium showed problems with exact georeferencing (offsets in the order of 1-2 SRTM pixels; presumably from pixel corner definition), so that the original SRTM from USGS is preferable over the CGIAR one unless a co-registration procedure (e.g. to ICESat) is performed. USGS SRTM description: http://dds.cr.usgs.gov/srtm/version2_1/Documentation.

The most actual release of ICESat can be freely downloaded or ordered from www.nsidc.org, or NASA WIST. Subsets can be ordered from NSIDC and are typically available for download after a few hours (days in worst case). Product description:
http://nsidc.org/data/icesat/index.html.

Radar altimeter data of the European Satellites ERS-1/2 and ENVISAT can be ordered and received via ESA'S EOLI portal (http://catalogues.eoportal.org/eoli.html). The data are free of charge for CCI projects.

Lack of access to ICESat, SRTM and the ASTER GDEM (in particular outside the SRTM coverage) would cause a significant problem to reach the project goals. However, we are not aware of any plans to restrict access to these datasets. Access to ASTER raw data is since launch under permanent discussion between NASA and JAXA, but we believe it is unlikely the access will be stopped for GLIMS users. In polar regions, the SPOT5 HRS SPIRIT DEMs are a (even preferable) alternative. The most relevant DEMs that have been created for these regions are already in the possession of GUIO and the consortium partners.

4.2 EO data for product validation

4.2.1 Data sources

Digital Elevation Models

External product validation will be through testing individual DEMs contributing to the elevation change product against each other. Thereby, elevations on glaciers require data from similar times, elevations outside glaciers not.

DEMs used in the elevation change product can be cross-validated from the product generation DEMs:

- ICESat, ASTER and SPOT5 HRS can be validated against each other over stable terrain and in many cases also over glaciers due to temporal overlap of the missions.
- SRTM can only be validated against the above DEMs over stable terrain due to the absence of temporal mission overlap. Of particular importance is to use only regions on flat ground for a direct comparison to avoid an elevation bias due to different cell sizes (Paul, 2008).

In addition high-resolution and high-accuracy DEMs are available for validation sites, partly with temporal overlap (validation of glacier and non-glacier elevations), partly without (validation of stable terrain):

- DEMs from airborne laserscanning. These DEMs are considered to be currently the most accurate glacier DEM possible, due to their high vertical and horizontal accuracy (dm-order), and their ability to provide elevations equally accurate over snow-coverd areas and snow-free ones.
- DEMs from aerial photogrammetry. Aerophotogrammetric DEMs have similar accuracy than those from laserscanning for snow-free areas, but are less reliable of snow areas. Else, their characteristics are similar to satellite stereo DEMs, except their higher resolution.

DEMs from national mapping agencies, which are also available for DEM validation are usually compilations of the one or both of the above to airborne DEM types.

A third type of validation DEMs are from high-resolution satellite stereo, with characteristics similar to the medium resolution spaceborne stereo DEMs and the airborne stereo DEMs. Most relevant for the Glaciers_cci project is thereby ALOS PRISM.

Altimetry products
ERS-1/2 and ENVISAT elevation change products will be validated against ICESat GLAS observations and DEM data obtained with the differencing approach and produced within the project, especially for mountain glaciers where few ICESat tracks are available.

In addition, the airborne measurements carried out during the IceBridge NASA mission over the Arctic will be used for the validation process. Based out of Thule and Kangerlussuaq, Greenland, this field campaign to monitor Greenland and Arctic sea ice focused on areas where glaciers have been undergoing rapid changes, including the Northwest Passage. A Ku-band radar altimeter was used on board of the NASA's DC-8 and P-3B aircraft. The data are available for periodic, ongoing campaigns from 26 March 2010 to the present via FTP through the NSIDC website. The operation IceBridge data products include also measurements carried out by the Airborne Thematic Mapper (ATM) laser over Arctic sea ice and Greenland, which are available for periodic, ongoing campaigns from 31 March 2009 to the present. Other available measurements for the validation process will be the ones acquired using the Airborne Topographic Mapper 3 (ATM3) over the Svalbard region (Fig. 4.1).

The instrument ATM3 used was a conical-scanning laser-ranging system with a pulse-repetition frequency of 5 kHz and a scan rate of 20 Hz in 2002 and 10 Hz in 1996. On the same region there are data available from the CRYOVEX (CryoSat Validation EXperiment) 2003 campaign which was a first comprehensive Arctic Ocean airborne and surface campaign, in support of the ESA satellite CryoSat. The airborne scanning laser (lidar) and radar measurements were carried out in the period April 1 to April 23, 2003. In support to the CryoSat-2 mission, ESA conducted extensive pre-launch validation campaigns by providing simultaneous overflights of surface experiments performed by Calibration, Validation and Retrieval Team (CVRT) members in Greenland, Canada, Svalbard and the Arctic Ocean in 2003, 2005, 2006, 2007 and 2008 (only the CryoVEX 2003 campaign is currently available at ESA). The most recent measurements of the Cryosat-2 validation activity were concentrated in April and May 2011 and were acquired in collaboration with the NASA IceBridge airborne campaign. A De Havilland Canada DHC-6-300 Twin Otter with an onboard laser scanner and a radar altimeter flew about 85 hours, covering about 20’000 km over central Greenland, Svalbard and the Fram Strait, Devon Island and Alert in northern Canada (Fig. 4.1).

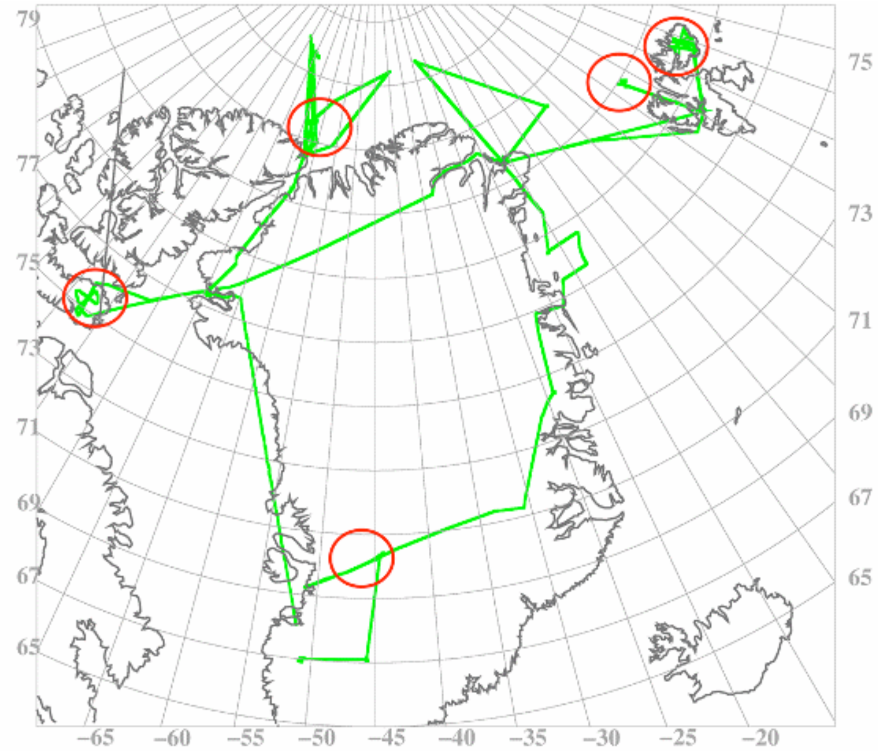

Fig. 4.1: Flight tracks from Twin Otter (credits: H. Skourup)

4.2.2 Data availability and access

For data availability and access of ASTER, SRTM, SPOT5 and ICESat see section 4.1.2. and 4.13, respectively. Aerophotogrammetric DEMs over nearly all Svalbard (small voids not affecting validation) with high reliability are from 1990 (Norwegian Polar Institute DEMs).

ALOS PRISM data suitable for glacier DEMs are only available for 2006 and 2007. After 2007, the gain settings have been modified so that the data are no longer useful over glaciers (though for ground not covered by snow). Suitable PRISM data for validation are only available on an opportunistic basis. No such scene is available for Svalbard, but two tracks over the Swiss Alps, and several ones over the Himalaya (though outside the European node ADEN) can be used for the project. The large processing effort needed makes PRISM DEMs to be the lowest priority for the DEMs under validation and they will thus only be applied in Glaciers_cci in a test case.

DEMs from laser scanning, aerophotogrammetry, and related national DEMs are usually restricted (exceptions: NED, CDED; see 3.3.1). However, suitable DEMs are already available by the consortium partners. They can be used for validation, but cannot be provided further. For validation purposes we have also access to high-resolution LIDAR data for Findelenglacier in Switzerland as well as to the new photogrammetric DEM (ADS-80 sensor) that is currently compiled by swisstopo. This DEM will be less precise than the LIDAR DEM, but available over larger regions and precise enough to be used for validation of other DEMs (cell size will be 2 m). The DEMs available for Svalbard are described in Nuth et al. (2010). Furthermore, high-resolution DEMs are available for some regions in the Himalaya, e.g. the Khumbu region (Bolch et al., 2011).

The datasets resulting from the above mentioned ESA airborne campaigns for validation of Cryosat-2 can be accessed by submitting a request on the ESA EO Campaigns data section of the EOPI website. The IceBridge data are available through NSIDC IceBridge data portal (http://nsidc.org/icebridge/portal).

4.3 Auxiliary data for product generation

4.3.1 Data sources

In order to compute glacier volume changes from elevation changes, hypsometric information is needed, based on as complete as possible DEMs. In addition to the above DEMs for product generation the following DEMs are suitable for hypsometry:

a) The ASTER GDEM (v1 and v2) is suitable because its deficiencies have little effect.
b) The void-filled version of the SRTM DEM from CGIAR can be used as (cf. Frey and Paul, in press) have shown.
c) Large-scale DEMs of non-global coverage such as NED, CDED, or DEMs from viewfinder work as well (see Table 3.9).

4.3.2 Data availability and access

Details of data availability and access are described above

4.4 Auxiliary data for product validation

In situ GNSS measurements (points and profiles) are available to GUIO in Svalbard (Ny Ålesund area and Austfonna) with cm-dm vertical accuracy, partly with and partly without temporal overlap with the DEMs to be validated. Mass balance measurements for numerous glaciers are available from WGMS. As the direct comparison between cumulative values from field based measurements of mass balance and geodetic volume changes is often not straight forward (e.g. Fischer, 2010), we will likely use such data more for comparison than for validation. For some glaciers stake measurements of elevation changes are also available (e.g. GNSS data from Svalbard), but these will mainly be used to validate the measurements from altimetry (annual basis) rather than the geodetic volume changes from DEM differencing. All the above mentioned data are freely available to the consortium.

5. Velocity

5.1 EO data for product generation

5.1.1 Introduction

Maps of glacier ice velocity from repeat pass spaceborne SAR data can be generated by applying three different processing techniques, including

- Differential SAR Interferometry (DInSAR),
- Coherent Image Cross-Correlation (Speckle Tracking), and
- Incoherent Amplitude Image Cross Correlation.

Although the different techniques itself make use of the same type data, they differ in the requirements regarding acquisition of the repeat pass SAR data (in particular the temporal repeat interval) in order to enable successful retrieval of ice velocities, in the retrieved component of the ice velocity vector and the sensitivity to displacement. The specific characteristics of the techniques, the specific requirements on the radar signal, and the capabilities in retrieving ice velocity are summarized in Table 5.1.

Method	Temporal Interval	Signal requirements	Displacement-accuracy	Special features
DInSAR	1 – 3 day	Coherence	High (fractions of one wavelength, several mm)	Velocity Component in Line of Sight Limitations due to decorrelation and shear
Speckle tracking: Cross-correlation of complex data or coherence images	1 to several days	Coherence, but less sensitive than DInSAR	Depending on spatial resolution, Fractions of a pixel	Provides two components of the velocity vector; works also in firn areas
Cross-correlation of incoherent amplitude or intensity images (feature tracking)	1 day (for fast glaciers) to several months	Non-coherent, but stable amplitude features	Depending on spatial resolution, Fractions of one pixel	Provides two components of the velocity vector; works well in regions with surface features (crevasses, etc.) and if speckle (coherence) is retained

Table 5.1: Techniques for retrieval of ice motion by repeat-pass SAR.

Strengths and weaknesses of the different techniques for ice motion retrieval are summarized in Table 5.1. DInSAR provides the highest sensitivity for observation of displacement, but temporal de-correlation often inhibits the application, in particular in case of multi-day time spans. De-correlation in zones of strong ice deformation (e.g. along glacier margins) is also a problem, impairing phase unwrapping and thus prohibiting to find a solution for ice velocity. Furthermore, DInSAR is only sensitive to the motion component in the radar look direction which requires the use of asc/desc image pairs and assumptions on the glacier flow in order to derive the full 3D velocity vectors.

The image cross-correlation techniques deliver two components of the velocity vector (slant range and azimuth) and can measure shifts at fractions of a pixel (Strozzi et al., 2002; de Lange et al., 2007). The accuracy of velocity measurement can be improved by using SAR data of longer time spans if the features (e.g. crevasses) are stable. In case of cross-correlation of complex data (speckle tracking or coherence tracking) a certain degree of coherence is required. In addition, phase unwrapping is not necessary so that de-correlation gaps can be bridged. Complex signal based cross-correlation (given a certain degree correlation) can also be applied in areas without obvious amplitude features which is often the case in accumulation areas. Incoherent amplitude cross-correlation (feature tracking) requires stable features, and therefore often fails in the upper reaches of glaciers (firn areas). On the other hand, it can be applied also in case of complete absence of coherence. Luckman et al. (2007) studied the potential of InSAR and feature tracking for Himalayan glaciers using ERS SAR data and found the two methods to be highly complementary, depending on flow rate and surface type. Feature tracking by ERS and Envisat ASAR is impaired by the relative low spatial resolution compared to the new X-band SAR sensors. This prohibits the application in zones of strong shear and deformation.

5.1.2 Data sources

Overview

A large number of repeat-pass SAR sensors have been and are currently used to derive ice motion. The most important missions since 1991 are summarized in Table 5.2 along with their main characteristics and their different orbital modes, which result in different repeat cycles. Current SAR sensors are in general operated without a systematic repeat pass acquisitions plan on a global scale, but acquisitions are done on demand. This requires the investigation of the availability of SAR data for the proposed key regions. In Table 5.3 a list of internet links to pages describing the specifications of the SAR sensor and their imaging modes is provided.

Satellite	Agency	Sensor	Geometric Resolution	Repeat-cycle	Swath Width	Availability
ERS-1	ESA	SAR C-Band: 5.3 GHz, VV Pol.	30 m	35 days, 3 days for selected periods, covering limited areas	100 km	Background data acquisition that covered glaciers well; 1991-2000
ERS-2	ESA	SAR C-Band: 5.3 GHz, VV Pol.	30 m	35 days, 3 days for selected periods, covering limited areas	100 km	Background data acquisition that covered glaciers well; 1995-2011
ERS-1/ERS-2 Tandem	ESA	SAR C-Band: 5.3 GHz, VV Pol	SAR C-Band: 5.3 GHz, VV Pol	1 day (2 satellites) and 35 days	100 km	Large data set 1995 - March 2000
ENVISAT	ESA	ASAR C-Band Polarisations: VV, HH, VV/HH, HV/HH, VH/VV	WSM mode: 150 m Image mode: 30 m	35 days	WSM: 400 km IM: 100 km	At first unsyste-matic acquisition, during IPY with a global strategy; since 2002
RADARSAT 1	CSA	SAR C-Band Polarisations: HH 8 beam modes	8 m - 100 m (dependent on mode)	24 days	45 - 500 km	No systematic acquisition apart from IPY; since 1995
RADARSAT 2	CSA	SAR C-Band Polarisations: HH, VV, HV VH 11 beam modes	3 m - 100 m (dependent on mode)	24 days	45 - 500 km	No systematic acquisition since 2008
TerraSAR-X	DLR	SAR X-Band Various modes	1 m to 18 m (dependent on mode)	11 days	10 - 100 km	No systematic data acquisition; since June 2007
TANDEM-X	DLR	SAR XBAND	1 m to 18 m (dependent on mode	11 day repeat cycle, in formation with TerraSAR-X single-pass interferometry	10 - 100 km	Acquisition planning by DLR; main task generation of DEMs; since June 2010
ALOS	JAXA	PALSAR L-Band: 1.27 GHz Polarisations: HH, VV, HH/HV, VV/VH	FBS mode: 10 m FBD mode: 20 m ScanSAR WB mode: 100 m	46 day	FBS: 70 km FBD: 70 km WB: 250 - 350 km	Global data acquisition strategy; since 2006, lost on 12 May 2011
COSMO-SkyMed 1-4	ASI	SAR-2000 X-Band fully polarimetric	Spotlight mode: 1 m Stripmap mode: 3 - 15 m ScanSAR: 30 - 100 m	1 day to 16 day	Spotlight mode: 10 km Stripmap mode: 30 - 40 km ScanSAR: 100 - 200 km	since 2007 (since 2010 :4 satellites)

Table 5.2: Overview of SAR sensors applied for ice motion retrieval. FBS - Fine Beam Single, FBD - Fine Beam Double.

Satellite	Link to Detailed Product Description
ERS 1 / 2	http://earth.esa.int/object/index.cfm?fobjectid=1016
Envisat ASAR	http://envisat.esa.int/pub/ESA_DOC/ENVISAT/ASAR/asar.ProductHandbook.2_2.pdf
Radarsat 1	http://gs.mdacorporation.com/includes/documents/R1_PROD_SPEC.pdf
Radarsat 2	http://gs.mdacorporation.com/includes/documents/RN-SP-52-1238 RS-2 Product Description 1-8_15APR2011.pdf
TerraSAR-X	http://www.infoterra.de/asset/cms/file/tx-gs-dd-3302_basic-product-specification-document_v1.7.pdf
ALOS PALSAR	http://earth.esa.int/object/index.cfm?fobjectid=5195
COSMO-SkyMed	http://www.e-geos.it/products/pdf/csk-product%20handbook.pdf

Table 5.3: Links to webpages with SAR product descriptions and corresponding sources.

The individual sensors

A timeline of data availability for all sensors is presented in Table 5.4. C-Band SAR data of ERS-1 are available since September 1991. Until March 1992 data were acquired in a 3 day repeat cycle (commissioning phase and ice phase), afterwards ERS data were acquired in 35 day repeat orbit. The Tandem Phase of ERS-1 and ERS-2 lasted from April 1995 to March 2000. The Envisat-ERS CInSAR tandem campaign was planned for two time periods with the main objective to measure glacier velocity and generation of DEMs (announced on 21 Jan 2010, at http://earth.esa.int/object/index.cfm?fobjectid=6754). First, from February to April 2010 target regions in Antarctica were chosen. The second period, lasting from July to September 2010 covers mainly regions at the northern hemisphere. Because of the slight difference in radar frequency, interferograms can be produced for the Envisat-ERS special InSAR experiments only for a part of the swath over comparatively level terrain. From 10 March 2011 to June 2011 the orbit of ERS-2 was changes, putting ERS-2 again into a 3 day repeat cycle.

ENVISAT ASAR repeat data are available from mid of 2002 to October 2010 in the nominal orbit. During this period altitude and inclination control was carried out in order to maintain the ground track within ± 1 km, with a repeat cycle of 35 days and 501 orbits per cycle. Since 1 November 2010 Envisat operates in the Extension Orbit, with 30 days repeat cycle and 431 orbits per cycle. Since 1 November 2010 only altitude control is performed, but no inclination control (i.e. correction of inclination drift) is applied. Therefore since November 2010 InSAR is in general no longer feasible, with exception of very few areas world-wide depending on the given orbit configuration.

The Canadian RADARSAT 1 was launched in November 1995, and is still operating in June 2011. The follow-on mission RADARSAT-2 was launched in December 2007.

The TerraSAR-X data acquisition started few days after the launch, in June 2007, providing X-band SAR data in numerous modes. For ice velocity monitoring the STRIPMAP mode is the most suitable mode. In June 2010 TanDEM-X (TerraSAR-X add-on for Digital Elevation Measurement), a second almost identical spacecraft to TerraSAR-X, was launched. The two satellites are flying in a closely controlled formation with typical distances between 250 and 500 m. The primary mission objective is the generation of a consistent global digital elevation model with an unprecedented accuracy according to the HRTI-3 specifications within about 3 years.

The Japanese ALOS satellite was launched in January 2006, PALSAR data are available since end of 2006. In April 2011 the ALOS satellite switched to a power-saving mode and no SAR data are acquired anymore. The sensor was declared dead on 12 May 2011.

The first of the 4 COSMO-Skymed satellites, carrying an X-band SAR, was launched in June 2007, since mid 2010 all 4 Satellite of the constellation are in space. The COSMO-Skymed constellation offers the possibility for data acquisitions with temporal baselines of 1, 8 and 16 days which are suitable for ice motion retrieval.

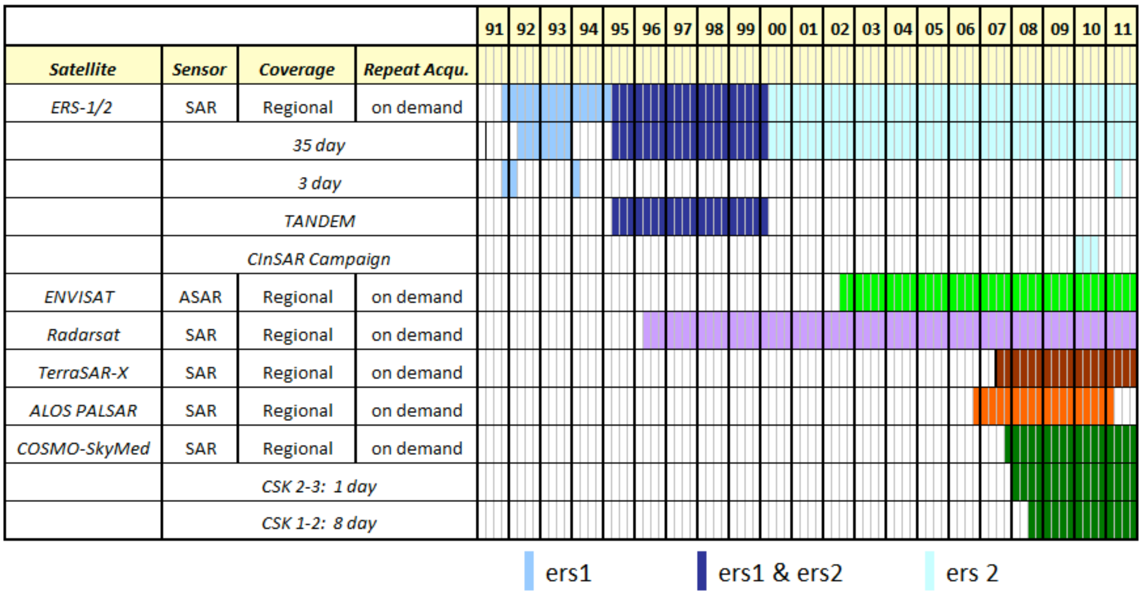

Table 5.4: Timeline of available SAR sensors and corresponding mission phases since 1991.

5.1.3 Data access

ERS-1/2, ENVISAT ASAR

Data of the European Satellites ERS-1/2 and ENVISAT can be ordered and received via ESA'S EOLI portal (http://catalogues.eoportal.org/eoli.html). The data are free of charge for CCI projects and can be ordered via CAT-1 project proposals.

RADARSAT

Radarsat Data can be ordered from 'MDA Geospatial services' at: http://www.mdacorporation.com. The price list for Radarsat 1 and Radarsat 2 data is on the web-page of MDA. Radarsat data over Svalbard are available to GUIO for validation and product generation (the data may not be passed to third parties, but the derived products are available).

TerraSAR-X

TerraSAR-X data are commercially available via DLR through a Web portal. Optionally TerraSAR-X data can also be ordered through INFOTERRA. TerraSAR-X data are in general acquired on demand. For research projects limited TerraSAR-X data sets are made either free of charge (project submitted before the satellite launch) or at a nominal fee per image. For Iceland and Switzerland some data are available from Gamma.

ALOS PALSAR

ALOS PALSAR data can be ordered via the EOLI portal of ESA. PALSAR can also be ordered directly from the PALSAR GDS (Ground Data Segment) at: https://ims1d.palsar.ersdac.or.jp/palsar_ims1_public/ims1/pub/en on a commercial basis. The price list can be downloaded from http://www.palsar.ersdac.or.jp/e/doc/pdf/PriceList_en.pdf. The PALSAR data required for the debris-cover mapping in the Himalaya have already been ordered via ESA.

COSMO-Skymed

COSMO-Skymed serves civil and military purposes. Data acquisition order and data delivery are handled commercially via e-GEOS (http://www.e-geos.it). For research projects limited COSMO-Skymed data sets are made available for research projects (AO) submitted before the launch. Enveo has some data available over Iceland that can be used by the CCI consortium.

Optical data

Optical image matching will mainly be based on orthorectified Landsat data and ASTER orthoimages. Access conditions for Landsat data are described in section 3.1.1. We will both use 30 m bands and, for Landsat 7 ETM+, 15 m-pan bands. The performance of both has to be tested in the algorithm development phase.

For ASTER data, access conditions are described in sections 3.1.1. and 3.3.1. We will use the orthoimages as part of the AST14DMO product. Vertical DEM errors translate into horizontal errors in orthoimages. These can be evaluated by comparing the band 3N and 3B orthoimages (see 4.1.1).

5.2 EO data for product validation

5.2.1. Data sources

Strict independent product validation for glacier velocities derived from air and space data is a difficult task because it would require reference measurements of exactly the same time. Due to short-term and seasonal velocity variations of glaciers, even small differences in the observation time window may introduce significant velocity differences. In addition, point measurements such as ground measurements represent a different surface area (points) than satellite measurements (averaging over pixel windows). Similar to above external validation approaches by reference measurements, a number of internal validation measures is available, but also all of these are not completely conclusive, and provide only indications.

We will therefore perform a whole set of internal and external validation measures:
External validation:

- Comparing satellite-derived velocity products against ground-based velocity measurements, for example continuous in-situ GNSS by GUIO on Kronebreen (Svalbard) and Iceland and GPS stations over Vestfonna (Svalbard).
- Comparing results from medium resolution satellites (e.g. ERS, ENVISAT, Radarsat, Landsat, ASTER) against those from high-resolution ones (e.g. Radarsat, TerraSAR-X, high-resolution optical).

- Comparing different medium resolution data against each other (Landsat5 /7, ASTER)

Internal validation:

- Matching of synthetic images (real images with analytic deformation and noise added)
- Reconstruction of first image from second image using measured displacements between first and second image, and comparison to real first image.
- Matching quality indicators such as signal-to-noise ratio or cross-correlation coefficient.

Validation of ice velocity fields from repeat pass SAR data is preferably done by intercomparison with in-situ point measurements of ice velocity. Below, the test site on Iceland (Fig. 5.1) and related data sets, proposed for the Round Robin, are described.

5.2.2 Data availability and access

TerraSAR-X data cannot be distributed freely. After negotiation with DLR it was agreed that the data licence can be extended to a limited number of persons in the Glaciers_cci project. The names need to be forwarded to the TSX mission manager (communication by A. Roth / TSX Mission Manager to T. Nagler / ENVEO; 1/7/2011). The available TerraSAR-X dataset is listed in Table 5.5. Temporal baselines between 11 and 33 days are possible which enables to investigate the accuracy as a function of the temporal baseline. The TerraSAR-X data sets are available at ENVEO and can be used by the Glaciers_cci consortium (but names have to be reported). Additional EO data for product validation are available for the Kronebreen test site on Svalbard (TerraSAR-X and Radarsat). Details are listed in Tables 5.6 and 5.7.

Acquisition YYYY/MM/DD	Acquisition Time UTC	Polarization	Strip	Track	Orbit
2008/08/04	07:31	HH	013	140	6319
2008/08/15	07:31	HH	013	140	6486
2008/08/26	07:31	HH	013	140	6653
2008/09/06	07:31	HH	013	140	6820

Table 5.5: Repeat pass TerraSAR-X scenes, descending, acquired in Stripmap mode STRIP 013 covering the validation site Breidamerkurjökull. TerraSAR-X data are available through TerraSAR-X (TSX) Science AO project HYD0096, for the PI and co-investigators of the HYD0096 project.

Acquisition YYYY/MM/DD	Acquisition Time UTC	Polarization	Orbit cycle	Abs .Orbit	Rel. Orbit
2008/03/25	15:16	VH,VV	26	4320	145
2008/04/27	15:16	HH,HV	29	4821	145
2008/05/08	15:16	HH,HV	30	4988	145

Table 5.6: Available TerraSAR-X data for product validation over Kronebreen.

Acquisition YYYY/MM/DD	Acquisition Time UTC	Polarization	Strip	Track	Orbit
2009/03/13	16:21	HH	Kronebreen	-	-
2009/04/06	16:21	HH	Kronebreen	-	-
2009/04/30	16:21	HH	Kronebreen	-	-
2009/02/04	14:20	HH	Aust/Vestfonna	-	-
2009/02/28	14:20	HH	Aust/Vestfonna	-	-

Table 5.7: Available Radarsat images over Kronebreen and Austfonna-Vestfonna.

5.3 Auxiliary data for product generation

5.3.1 Data sources

The following auxiliary data are needed for product generation:

- Digital elevation models
- Glacier outlines (optional)

5.3.2 Data availability and access

Outlines for test glaciers:

- will be generated for the selected glaciers within the project
- taken from the public GLIMS data base (if available)

The SRTM DEM and GDEM is freely available, but the SRTM DEM only cover the test site Himalaya / Karakoram. For Svalbard the DEM of the Norwegian Polar Institute (NPI) is available to GUIO, for Iceland DEM data are available to Enveo.

5.4 Auxiliary data for product validation

5.4.1 Data sources, availability and access

Test site Iceland

The glacier Breidamerkurjökull, Iceland, is proposed as one test site for the validation of ice motion fields derived by the incoherent amplitude correlation (Feature Tracking) method. Breidamerkurjökull is an outlet glacier of the ice cap Vatnajökull, located at 64.13°N and 16.30°W. The elevation of the glacier ranges from about 200 m a.s.l. to 2000 m a.s.l. The glacier drains from the plateau of the ice cap towards the South. The central part of the glacier front calves into the lake Jökulsárlón, which evolved after retreat from the maximum glacier extent in the 1890s (Björnsson et al., 2001). In Fig. 5.2 an overview of Breidamerkurjökull terminus is shown. The University of Iceland installed three permanent GPS stations monitoring continuously the ice motion. The locations of the GPS stations are indicated as red circles in Fig. 5.1. They are located on the lower part of Breidamerkurjökull, close to the centre flow line. The central part of Breidamerkurjökull calves into the frontal lake Jökulsárlón and has the highest ice velocities. East and west of this central region the ice motion is significantly reduced (Howat et al., 2008).

Position measurements are recorded at an automated GPS station on location BMJ2 at 15 seconds sampling interval (Table 5.8). To prepare the data for validation, post-processing of the GPS measurements is performed. As a first step differential GPS processing is applied. In order to reduce noise the 15 seconds data set was filtered with a moving window of 2 days and a manual quality control was performed. The time series of the post-processed GPS data was used to calculate ice motion for the corresponding time intervals of the TerraSAR-X acquisitions listed in Table 5.5. The error in the displacement measurement of BMJ2 is negligible for the 11-day repeat cycle of TerraSAR-X (personal com. E. Magnússón, Univ. Iceland, 2010, 2011). Ice speed fields with geodetic measurements done during 2007-2010 were published by Pohjola et al. (in press) and can be employed for validation within our project.

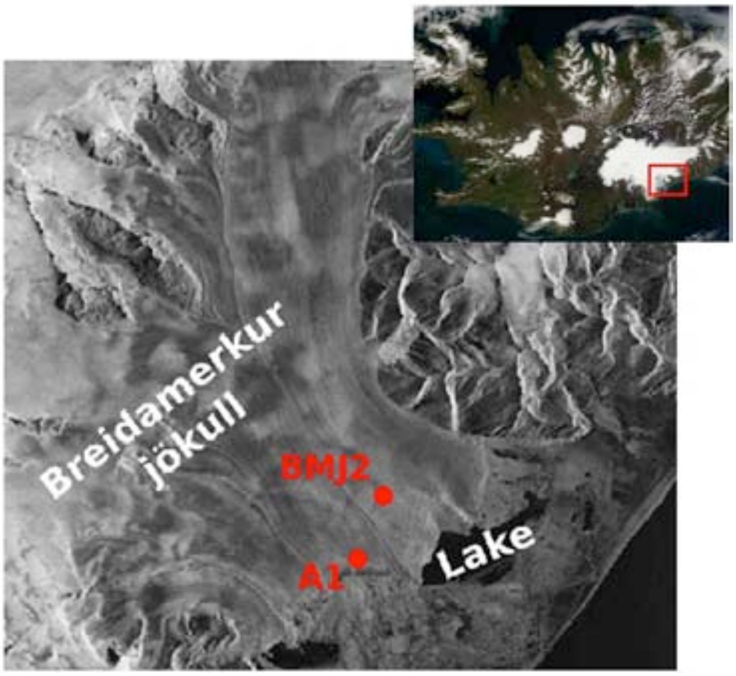

Figure 5.1: Overview of the validation site Breidamerkurjökull, Vatnajökull ice cap, Iceland. Red circles indicate the location of GPS station BMJ2 and the meteorological station A1. The inset shows the location of Breidamerkurjökull at the south-east part of Vatnajökull. The ice of the glacier terminus drains into the frontal lake Jökulsárlón.

Figure 5.2: GPS Station BMJ2 with auxiliary energy supply by solar panels and batteries at Breidamerkurjökull facing southwards to the Atlantic Ocean (courtesy Eyjólfur Magnússon, Institute of Earth Sciences, University of Iceland).

Station ID	Location	Acquisition Period	Instrument Description
BMJ2	Lat Lon	2008/08/04 – 2008/09/06	Trimble NetRS GPS, 15 sec. acquisitions
A1	Lat Lon	2008/08/04 – 2008/09/06	Sonic Ranger measuring ice ablation

Table 5.8: Available in-situ data at Breidamerkurjökull. Approximate locations of the GPS stations is shown in Fig. 5.1.

Test site Svalbard

Vestfonna is selected as further validation site. Vestfonna was a major target of multi-disciplinary field campaigns launched within the, KINNVIKA project during IPY. The geodetic measurements were done both as static surveying of stakes and as continuously recording GPS stations (Fig. 5.3).

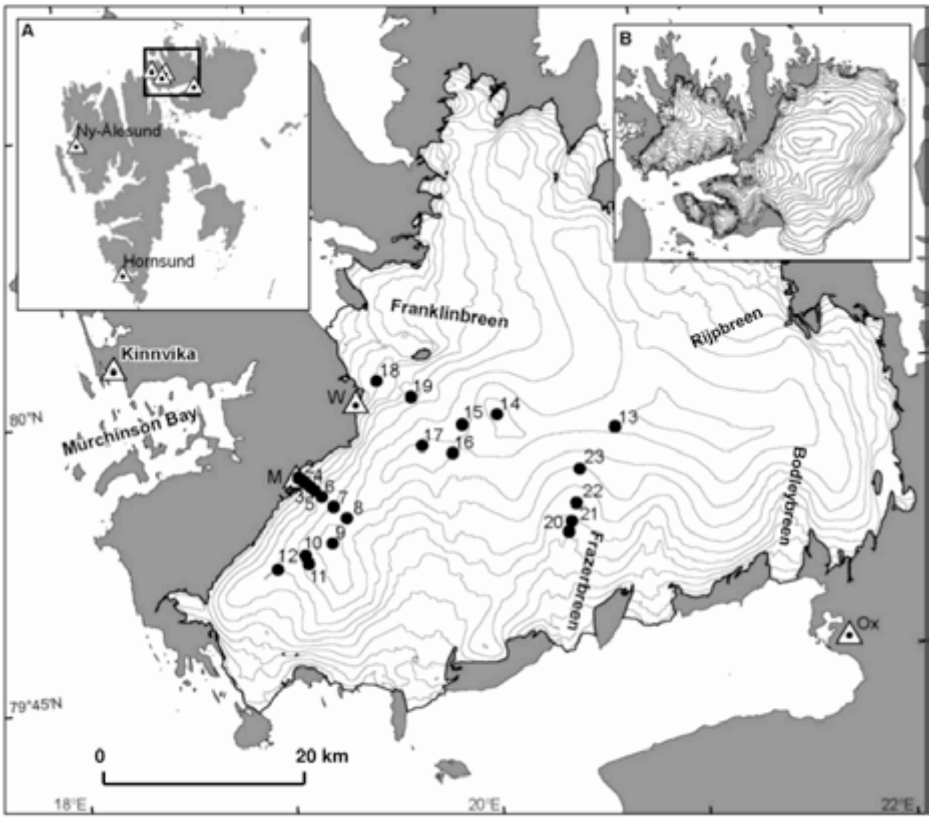

Fig. 5.3: Svalbard, Nordausdandet and the ice cap Vestfonna. Elevation- and coast line contours are from the Norwegian Polar Institute DEM. The elevation contour spacing is 500 m. The black dots mark the position markers used for our DGPS surveys. The triangular symbols are the fixed points / base stations. The letter at each fixed point / base station refers to the first letter of its name. The Malti- and Weasel lobes are the bulging features with fronts ending at the base stations marked with M and W respectively. Donckerfjellet is the terrain SW of Franklinbreen, where the Weasel base station is marked. Inset a) show the base stations and inset b) show the topography of all the ice caps on Nordaustlandet. The contours are from the NPI DEM. Taken from Pohjola et al. (in press).

Annual velocity measurements (from stakes) are available on Kronebreen since 2003, mainly above the lower crevassed zone. Since 2007, code based GPS receivers have been placed in the lower crevassed zone. From 2011, continuous dual frequency GPS receivers have been monitoring velocities close to the ELA of the glacier. On Austfonna, code based receivers have been monitoring velocity since 2008 over 2 basins, Duvebreen and Basin 3. Since 2011, continuous dual frequency GPS has also been operated on these basins. All GPS data are available to GUIO. The in situ GNSS measurements over Svalbard are already described in section 4.4 as they will also be used to validate the elevation change product.

References

Abermann, J., A. Fischer, A. Lambrecht and T. Geist (2010): On the potential of very high-resolution repeat DEMs in glacial and periglacial environments. The Cryosphere, 4, 53-65.

Berthier E., E. Schiefer, G.K.C. Clarke, B. Menounos, and F. Remy (2010): Contribution of Alaskan glaciers to sea level rise derived from satellite imagery. Nature Geoscience, 3(2), 92-95.

Björnsson, H., F. Pálsson and S. Gudmundsson (2001): Jökulsárlón at Breidamerkursandur, Vatnajökull, Iceland: 20th century changes and future outlook. Jökull, 50, 1-18.

Bolch, T., Pieczonka, T. and D.I. Benn, (2011): Multi-decadal mass loss of glaciers in the Everest area (Nepal, Himalaya) derived from stereo imagery. The Cryosphere, 5, 349-358.

Brenner, A. C., DiMarzio, J. R., & Zwally, H. J. (2007). Precision and accuracy of satellite radar and laser altimeter data over the continental ice sheets. *IEEE Transactions on Geoscience and Remote Sensing , 45* (2), 321-331.

Citterio, M., F. Paul, A.P. Ahlstrøm, H.F. Jepsen and A. Weidick (2009): Remote sensing of glacier change in West Greenland: accounting for the occurrence of surge-type glaciers. Annals of Glaciology, 50 (53), 70-80.

de Lange, R., A. Luckman and T. Murray (2007): Improvement of satellite radar feature tracking for ice velocity derivation by spatial frequency filtering. IEEE Transactions on Geoscience and Remote Sensing, 45, 2309-2318.

ESA (2008): ESA Online News Bulletin (Jan 2008). ENVISAT RA-2 S-band anomaly 23 January 2008. Online at: http://earth.esa.int/object/index.cfm?fobjectid=5483

ESA (2010): ESA's Earth observation third party missions - Data access guide. Online at: http://earth.esa.int/TPMDAG

Farr, T.G., et al. (2007): The Shuttle Radar Topography Mission, Reviews of Geophysics, 45, RG2004.

Fischer, A. (2010): Comparison of direct and geodetic mass balances on a multi-annual time scale, The Cryosphere, 5, 107-124

Frey, H. and F. Paul (in press): On the suitability of the SRTM DEM and ASTER GDEM for the compilation of topographic parameters in glacier inventories. International Journal of Applied Earth Observation and Geoinformation.

Frey, H., F. Paul and T. Strozzi (subm.): Compilation of a glacier inventory for the western Himalayas from satellite data: Methods, challenges and results. Remote Sensing of Environment.

Glaciers_cci (2011a): User Requirements Document (URD). Prepared by the Glaciers_cci consortium, 45 pp.

Glaciers_cci (2011b): Product Specification Document (PSD). Prepared by the Glaciers_cci consortium, XX pp.

Glaciers_cci (in prep.): Product Validation Plan (PVP). Prepared by the Glaciers_cci consortium, XX pp.

Hayakawa, Y.S., T. Oguchi, and Z. Lin (2008): Comparison of new and existing global digital elevation models: ASTER G-DEM and SRTM-3. Geophysical Research Letters 35, L17404.

Hiranoa, A., R. Welch and H. Lang (2003): Mapping from ASTER stereo image data: DEM validation and accuracy assessment. ISPRS Journal of Photogrammetry & Remote Sensing, 57, 356-370.

Howat, I.M., S. Tulaczyk, E. Waddington and H. Björnsson (2008): Dynamic controls on glacier basal motion inferred from surface ice motion. Journal of Geophysical Research, 113, F03015.

Kääb, A. (2002): Monitoring high-mountain terrain deformation from repeated air- and spaceborne optical data: examples using digital aerial imagery and ASTER data. ISPRS Journal of Photogrammetry & Remote Sensing, 57 (1-2), 39-52.

Kääb, A. (2008): Glacier volume changes using ASTER satellite stereo and ICESat GLAS Laser Altimetry. A Test Study on Edgeøya, Eastern Svalbard. IEEE Transactions on Geoscience and Remote Sensing, 46 (10), 2823-2830.

Lambrecht, A. and M. Kuhn, 2007: Glacier changes in the Austrian Alps during the last three decades, derived from the new Austrian glacier inventory. Annals of Glaciology, 46, 177-184.

Le Bris, R., Paul, F., Frey, H. and Bolch, T. (2011): A new satellite-derived Glacier Inventory for Western Alaska. Annals of Glaciology, 52 (59), 144-153.

Legresy, B., F. Papa, F. Remy, G. Vinay, M. van den Bosch, O.-Z. Zanife (2005): ENVISAT radar altimeter measurements over continental surfaces and ice caps using the ICE-2 retracking algorithm. Remote Sensing of Environment, 95(2), 150-163.

Luckman, A., D. Quincey and S. Bevan (2007) The potential of satellite radar interferometry and feature tracking for monitoring flow rates of Himalayan glaciers. Remote Sensing of Environment, 111, 172-181.

Nuth C. and A. Kääb (2011): Co-registration and bias corrections of satellite elevation data sets for quantifying glacier thickness change. The Cryosphere, 5, 271-290.

Nuth C., G. Moholdt, J. Kohler, J.O. Hagen and A. Kääb (2010): Svalbard glacier elevation changes and contribution to sea level rise. Journal of Geophysical Research, 115, F01008.

Paul, F. (2008): Calculation of glacier elevation changes with SRTM: Is there an elevation dependent bias? Journal of Glaciology, 55 (188), 945-946.

Paul, F. and A. Kääb (2005): Perspectives on the production of a glacier inventory from multispectral satellite data in the Canadian Arctic: Cumberland Peninsula, Baffin Island. Annals of Glaciology, 42, 59-66.

Paul, F. and W. Haeberli (2008): Spatial variability of glacier elevation changes in the Swiss Alps obtained from two digital elevation models. Geophysical Research Letters, 35, L21502.

Paul, F. and L.M. Andreassen (2009): A new glacier inventory for the Svartisen region, Norway, from Landsat ETM+ data: challenges and change assessment. Journal of Glaciology, 55 (192), 607-618.

Paul, F., C. Huggel, A. Kääb and T. Kellenberger (2003): Comparison of TM-derived glacier areas with higher resolution data sets. EARSeL Workshop on Remote Sensing of Land Ice and Snow, Bern, 11.-13.3.2002. EARSeL eProceedings, 2, 15-21.

Pohjola, V.A., P. Christoffersen, L. Kolondra, J.C. Moore, R. Pettersson, M. Schäfer, T. Strozzi, and C.H. Reijmer (in press): Spatial distribution and change in the surface ice-velocity field of Vestfonna ice cap, Nordaustlandet, Svalbard, 1995-2010 using geodetic and satellite interferometry data. Geografiska Annaler.

Raup, B.H., H.H. Kieffer, T.M. Hare and J.S. Kargel (2000): Generation of data acquisition requests for the ASTER satellite instrument for monitoring a globally distributed target: Glaciers. IEEE Transactions on Geoscience and Remote Sensing, 38 (2), 1105-1112.

Rémy, F. and S. Parouty (2009): Antarctic Ice Sheet and Radar Altimetry: A Review. Remote Sensing, 1, 1212-1239.

Reuter, H.I., A. Nelson, A. Jarvis (2007): An evalutation of void filling interpolation methods for SRTM data. International Journal of Geographic Information Science, 21, 983-1008.

Rignot, E., K. A. Echelmeyer, and W. Krabill (2001), Penetration depth of interferometric synthetic-aperture radar signals in snow and ice, Geophys. Res. Lett., 28(18), 501-504.

Roca, M., Laxon, S., & Zelli, C. 2009. The EnviSat RA-2 Instrument Design and Tracking Performance. IEEE Transactions on Geoscience and Remote Sensing, 47(10), 3489–3506. Resti, A., Benveniste, J., Roca, M., & Levrini, G. 1999a (JUN). The Envisat Radar Altimeter System (RA-2). ESA Bulletin. ESTEC.

Rodríguez, E., C.S. Morris and J. E. Belz (2006): A Global Assessment of the SRTM Performance, Photogrammetric Engineering & Remote Sensing, 72 (3), 249-260.

Rosmorduc, V., Benveniste, J., Bronner, E., Dinardo, S., Lauret, O., Maheu, C., Milagro, M. and Picot, N. (2011): Radar Altimetry Tutorial (Editors: J. Benveniste and N. Picot) (online at: http://earth.eo.esa.int/brat/html/general/overview_en.html)

Schiefer, E., B. Menounos and R. Wheate (2007): Recent volume loss of British Columbian Glaciers, Canada. Geophysical Research Letters, 34, L16503.

Strozzi T., A. Luckman, T. Murray, U. Wegmüller and C. Werner (2002): Glacier motion estimation using SAR offset-tracking procedures. IEEE Transactions on Geoscience and Remote Sensing, 40, 2384-2391.

Tucker, C.J., D.M. Grant and J.D. Dykstra (2004): NASA's global orthorectified Landsat data set. Photogrammetric Engineering and Remote Sensing, 70 (3), 313-322.

USGS (2008): Landsat Data Policy. Released 17 January 2008 by USGS and NASA. Online at http://landsat.usgs.gov/documents/Landsat_Data_Policy.pdf

Abbreviations

ALOS	Advanced Land Observing Satellite
ASTER	Advanced Spaceborne Thermal Emission and Reflection radiometer
CCI	Climate Change Initiative
CDED	Canadian Digital Elevation Dataset
CGIAR	Consultative Group on International Agricultural Research
CRG	Climate Research Group
DARD	Data Access Requirements Document
DEM	Digital Elevation Model
DTED	Digital Terrain Elevation Data
ERS	European Remote Sensing Satellite
ESA	European Space Agency
ETM+	Enhanced Thematic Mapper plus
FCDR	Fundamental Climate Data Record
GDEM	Global DEM
GLIMS	Global Land Ice Measurements from Space
GLS	Global Land Survey
InSAR	Interferometric SAR
L1T	Level 1 T (terrain corrected)
LDCM	Landsat Data Continuity Mission
MSI	Multi Spectral Imager
NASA	National Aeronautic and Space Administration
NED	National Elevation data
OLI	Operational Land Imager
PALSAR	Phased Array type L-band SAR
PSD	Product Specifications Document
PVP	Product Validation Plan
RMSE	Root Mean Square Error
SAR	Synthetic Aperture Radar
SoW	Statement of Work
SPOT	System Pour l'Observation de la Terre
SRTM	Shuttle Radar Topography Mission
SWIR	Short Wave InfraRed

TM	Thematic Mapper
URD	User Requirements Document
USGS	United States Geological Survey
UTM	Universal Transverse Mercator
WGMS	World Glacier Monitoring Service

Appendix 1 (Internet links)

Data access

Data	URL for Download
Landsat	http://glovis.usgs.govor http://earthexplorer.usgs.gov
ASTER (satellite data)	https://wist.echo.nasa.gov/api/
SPOT	http://catalog.spotimage.com or http://eoli.esa.int
HR Sat. (screen-shot)	http://maps.google.com
HR Sat. (procurement)	http://www.npoc.ch (IRS, Quickbird, Ikonos/Geoeye, etc.)
Aerial photogr. (Norway)	http://norgeibilder.no
Aerial photogr. (Switzerl.)	http://map.lubis.admin.ch/
ERS-1/2 & ENVISAT	http://catalogues.eoportal.org/eoli.html
Radarsat	http://www.mdacorporation.com
TerraSAR-X	http://www.infoterra.de/direct-access-services (ordering)
ALOS PALSAR	https://ims1d.palsar.ersdac.or.jp/palsar_ims1_public/ims1/pub/en
COSMO-Skymed	http://www.e-geos.it
SRTM (USGS)	http://dds.cr.usgs.gov/srtm/version2_1/SRTM3
SRTM (CGIAR)	http://srtm.csi.cgiar.org/selection/inputCoord.asp
GDEM (ASTER)	http://www.gdem.aster.ersdac.or.jp/
NED (USGS)	http://seamless.usgs.gov/ned1.php
CDED (Canada)	http://www.geobase.ca/geobase/en/data/cded/
viewfinder	http://www.viewfinderpanoramas.org/dem3.html
SPIRIT (SPOT)	http://polardali.spotimage.fr:8092/IPY/dalisearch.aspx
ASTER (AST14DMO)	https://lpdaac.usgs.gov/lpdaac/products/aster_products_table
GLS DEM (USGS)	ftp://ftp.glcf.umd.edu/glcf/GLSDEM/

Data descriptions

Satellite	URL for detailed descriptions
Satellites (general)	http:// database.eohandbook.com/database/missionindex.aspx
Landsat	http://landsathandbook.gsfc.nasa.gov/
ASTER	http://asterweb.jpl.nasa.gov/content/03_data/04_documents/aster_user_guide_v2.pdf
SPOT	http://www.spotimage.com/web/en/229-the-spot-satellites.php
ERS 1 / 2	http://earth.esa.int/object/index.cfm?fobjectid=1016
Envisat ASAR	http://envisat.esa.int/pub/ESA_DOC/ENVISAT/ASAR/asar.ProductHandbook.2_2.pdf
Radarsat 1	http://gs.mdacorporation.com/includes/documents/R1_PROD_SPEC.pdf
Radarsat 2	http://gs.mdacorporation.com/includes/documents/RN-SP-52-1238 RS-2 Product_ Description 1-8_15APR2011.pdf
TerraSAR-X	http://www.infoterra.de/asset/cms/file/tx-gs-dd-3302_basic-product-specification-document_v1.7.pdf
ALOS PALSAR	http://earth.esa.int/object/index.cfm?fobjectid=5195
COSMO-SkyMed	http://www.e-geos.it/products/pdf/csk-product%20handbook.pdf
ICESat (GLAS)	http://nsidc.org/data/icesat
SRTM DEM	http://srtm.usgs.gov
CGIAR DEM	http://www.cgiar-csi.org/
GDEM	http://www.ersdac.or.jp/GDEM/E/2.html